Winter 2007

Investigation of a Possible Lead-Lag Relationship Between the Innuitian and Laurentide Ice Sheets, Arctic Canada

Paula Zimmerman
Old Dominion University

INVESTIGATION OF A POSSIBLE LEAD-LAG RELATIONSHIP BETWEEN THE INNUITIAN AND LAURENTIDE ICE SHEETS, ARCTIC CANADA

by

Paula Zimmerman
B.S. December 2001, Michigan Technological University

A Thesis Submitted to the Faculty of
Old Dominion University in Partial Fulfillment of the
Requirement for the Degree of

MASTER OF SCIENCE

GEOLOGY

OLD DOMINION UNIVERSITY
December 2007

Approved by:

Dennis Darby (Director)

Jens Bischof (Member)

G. R. Whittecar (Member)

ABSTRACT

INVESTIGATION OF A POSSIBLE LEAD-LAG RELATIONSHIP BETWEEN THE INNUITIAN AND LAURENTIDE ICE SHEETS, ARCTIC CANADA

Paula Zimmerman
Old Dominion University, 2007
Director: Dr. Dennis Darby

Peaks of iron-rich grains in Arctic Ocean sediment cores matched to the Laurentide and Innuitian Ice Sheets appear to show a lead-lag relationship during the Late Pleistocene when grain abundances are plotted against time and depth below sea floor. Cores from across the Arctic have been analyzed to determine if this is the case. Of the six IRD events identified, the Innuitian leads 68% of the time with 26% of events in all cores occurring simultaneously. The Innuitian seems to lead 33.3% of the time when peaks from the Innuitian and Laurentide occur within close proximity (less than 1 cm), with 41.7% of the Innuitian and Laurentide peaks occurring simultaneously. Innuitian IRD events lasted an average of 1.5 to 3 kyr, while Laurentide events lasted an average of 1.1 to 2 kyr. A particularly well-dated event around 18 ka in PS1230 shows the Laurentide lagging the Innuitian by around 250 years. This short response time suggests that instabilities can be rapidly transmitted from one coalesced ice sheet to another.

ACKNOWLEDGEMENTS

There are many people who have contributed to the successful completion of this thesis. I would like to thank the members of my committee for their guidance, Steve Herman for his many hours at the microprobe, and Joshua Luther for simplifying the SAS routine used in this study. I extend a special thanks to Dr. Dennis Darby for his patience and guidance throughout this project.

TABLE OF CONTENTS

LIST OF TABLES

LIST OF FIGURES

LIST OF FIGURES CONTINUED

LIST OF FIGURES CONTINUED

Figure Page

CHAPTER I
INTRODUCTION

Ice rafted debris (IRD) events from the Innuitian ice sheet (IIS) and Laurentide ice sheet (LIS) during the Late Wisconsin (Figure 1) show an apparent asynchronicity (Darby et al., 2002). Innuitian events seem to occur first, followed by Laurentide events. This asynchrony was first discovered in a Fram Strait boxcore, PS1230, with peaks in detrital Fe oxide grain abundances matched to these two sources of glacial IRD (Figure 2, Darby et al. 2002). This core, located in the center of the ice export zone of Fram Strait is an excellent indicator of past ice transport from the Arctic Ocean.

The exact relationship between the IIS and LIS ice-rafted events is unknown beyond the fact that IRD events seem to occur from the Innuitian prior to their occurrence from the Laurentide Ice Sheet (Darby et al., 2002). Because of the limitation of radiocarbon dating and slow deposition rates in most of the cores used (Darby et al., 2002), the difference between the peaks in Fe grains from the Innuitian and Laurentide sources ranged from a few hundred years to 2,000 years. The time lapse between these events is important, but due to the vagaries of radiocarbon dating and the generally low deposition rates in the cores analyzed thus far, the resolution is unlikely to improve. If smaller ice sheets like the IIS were able to influence the ice calving production of the LIS, one would expect the IIS to occur immediately prior to each LIS event. If this can be established, the case is strengthened for a possible cause and effect such that IIS

The model journal for this thesis is *Paleoceanography*.

Figure 1. Paleogeography of the Arctic Ocean during the Last Glacial Maximum. Base map – IBCAO (Jakobsson et al., 2000a). Limits of major ice sheet are from Dyke et al., (2002) and Svendsen et al., (2004a;b). During earlier glaciations the Eurasian Ice Sheet was more extensive on its Siberian side (Darby et al., 2006).

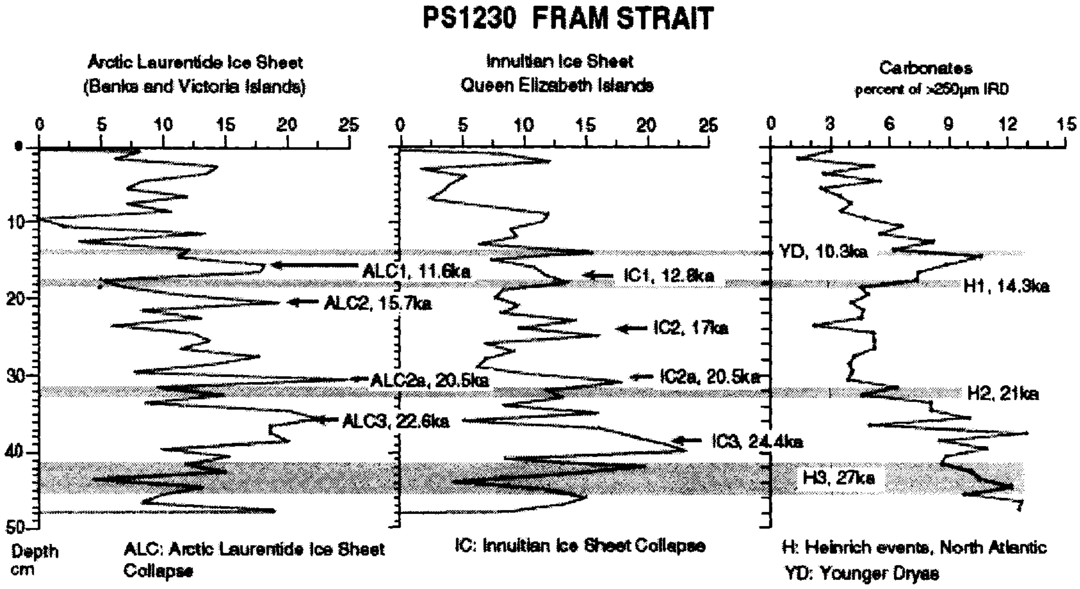

Figure 2. Fe grain matches to the Arctic Laurentide Ice Sheet (LIS, Banks Island source area) and the Innuitian Ice Sheet (IIS, Queen Elizabeth Islands source area) in core PS1230 from Fram Strait, displaying lead-lag relationship between IIS and LIS IRD events (Darby et al., 2002). Units on X-axis are weighted percent of Fe rich grains matched to the source area. These sources, especially the LIS source (Victoria Island) contain abundant carbonate rocks and counts on this lithic grain type in the >250 µm fraction supports the Fe grain matches. The blue shaded bands correspond to Heinrich Layers in the North Atlantic and these seem to lag both the IIS and LIS events. Ages are calendar ages in kyr.

calving events function as a trigger for increased calving of the LIS. How this smaller ice sheet could do this is an important issue in ice sheet dynamics and possibly climate change.

Problem

The Arctic is thought to have a significant effect on global climate yet many of the forcing mechanisms and interactions between different components of the climate system are poorly understood. (Alley, 1995). For instance, we do not know the duration, extent, or controlling mechanisms of LIS and IIS IRD events. The possibility of a lead-lag relationship between the Innuitian and Laurentide Ice Sheets raises several questions;

1. What is the timing and duration of the IRD events? In other words, do these IRD events represent a rapid collapse of the ice sheet and if so, how rapid?
2. If there is a lead-lag relationship between IIS and LIS collapse events, what might this relationship mean?
3. Could the IIS be acting as a buttress for the LIS?

Resolving these questions would give a much clearer picture of the relationship between the IIS and LIS in the Late Wisconsin, and will contribute to our general understanding of interactions between small and large ice sheets. By examining the abundance of ferromagnetic grains matched to specific ice sheet sources in the 45 to 250-μm-size fraction in sediment cores from the Arctic Ocean, relationships between the relative timing of IIS and LIS IRD events might be resolved. There has been much debate over what causes IRD events, with explanations typically involving either glacial mechanics, sensitivity to changes in climate, or changes in ocean circulation (MacAyeal, 1993; Bond and Lotti, 1995; Johnson and Lauritzen, 1995; Fronval et al., 1995; Marshall and Clarke, 1997; Scourse et al., 2000; Grousset et al., 2000; Hulbe et al., 2005). If each Innuitian event is followed by a Laurentide event, it would suggest, but not prove, that the Innuitian Ice Sheet somehow affected the calving rate of the Laurentide Ice Sheet. Perhaps changes in the calving rate occurring in the smaller ice sheet were somehow transmitted to the larger one. If only some Innuitian events were followed by Laurentide events, it would suggest that the Innuitian was more sensitive perhaps to environmental changes or ice dynamics promoting increased calving, but that changes in the IIS could only be transmitted to the LIS at such a time when the LIS was susceptible to such influences on its calving rate. Though the IIS events might trigger changes in the LIS, they would be one factor in many influencing calving. For instance, the IIS must have reached a maximum volume after which any additional accumulation must result in purging (MacAyeal, 1993). Alternatively, the IIS might have experienced a change in basal conditions that caused surging (Stokes and Clark, 2001), or changes in ocean temperature might have acted to melt buttressing ice shelves (Hulbe et al., 2005).

Examining the abundance of grains from individual fiords during an IRD event from the IIS can give some indications as to how the IIS purges ice or collapses. If the majority of grains in any given event came from one particular fiord, it would mean that this fiord was more susceptible to calving than the others, possibly due to loss of a buttressing ice shelf or the establishment of an ice stream in this ice sheet. Ice shelves and streams are very important to the stability of an ice sheet (Stokes and Clark, 2001; Hulbe et al., 2005) and the ability to demark these features would give a much clearer view of the overall sensitivity of the IIS to collapse or surging processes. A lack of grains from a given glaciated area could mean either that the area was not occupied by ice at the time, or the ice was not calving. This paper will present additional data on the cores used by Darby et al., (2002) as well as some additional cores to clarify the relationship between the IIS and LIS Fe grain matches during rapid calving events defined by peaks in Fe grains matched to either or both of these ice sheets.

The role of sea ice in IRD transport during glacial intervals is still poorly understood. This is thought to be possibly the most important transport agent in the Arctic Ocean today (Reimnitz et al., 1998; Darby et al., 2003). The importance of this transport process during glacial intervals is unknown. Lower sea levels at these times would expose the expansive Siberian shelves and should have drastically reduced the sea ice entrainment that occurs on these submersed shelves today. There is some evidence that rafting by sea ice might be very important during these times when icebergs were much more abundant (Darby et al., 2002), but much more needs to be done to establish the relative importance of iceberg versus sea ice sediment transport during glacial intervals. This paper will examine the abundance of Fe grains matched to areas known to be unglaciated during the last couple of glacial intervals and compare their abundance to Fe grains from known glacial areas for these intervals. The duration of Fe grain peaks from glaciated areas will also be examined. Very wide peaks may be reflecting the rafting of Fe grains by sea ice as well as transport by glacial bergs. Identifying these peaks will be important in order to distinguish which events are the result of rapid ice sheet collapse and which are the result of slower depositional processes such as melt out from sea ice.

Arctic Canada at the Last Glacial Maximum, Late Pleistocene, and Early Holocene

The Last Glacial Maximum (LGM) occurred around 20 ka during the time of Oxygen Isotope Stage 2 (OIS-2, 25-10 ka) in the last part of the Wisconsinan (Weichselian) glacial, which was 115-10 ka. (Dyke et al., 2002). During most of OIS-2, the North American ice sheets were coalesced and ice margins extended to the continental shelf (Figure 2).

During OIS-2 the IIS covered most of the Queen Elizabeth Islands, Arctic Canada (Blake, 1970; Blake, 1992; Blake et al., 1992; Blake, 1997; England, 1998; England, 1999). The extent of the IIS was debated until recently, but the concept of a relatively larger, coalesced IIS has since been accepted as more likely than many isolated ice caps on each island. At the LGM, the IIS coalesced with the Greenland Ice Sheet (GIS) along Nares Strait and coalesced with the LIS along Parry Channel for a distance of at least 1280 km (Dyke et al., 2002; England, 1998; England et al., 2006). Darby et al. (2002) estimated the volume of the Arctic component of the LIS to be approximately 1.3×10^6 km^3. The exact size of the IIS and Arctic LIS are unknown, as glacial margins are now submerged.

Around 11,000 years BP the final deglaciation of the Arctic portion of the LIS and IIS began in the Canadian Arctic (England, 1998). There were probably several rapid purges of icebergs from the IIS and LIS during MIS 2-4 primarily based on the marine record (Darby et al., 2002) but also on ages of tills at outlets for LIS ice streams on Banks Island and Victoria Island (Stokes et al., 2005). Retreat of the LIS from its northern margin may have begun as early as 16,200 ± 150 ^{14}C years BP (Dyke et al., 2002). Recession times are uncertain for the IIS because the northern margin of the IIS, which is now probably submerged, has not been conclusively demarked and dated. Pulses of IRD linked to both the LIS and IIS have been found in Fram Strait and Arctic cores at 18 and 18.2 ka cal. yrs. (15.7 &15.9^{14}C kyr) ± 150, respectively; and another at about 15 ka Cal. yrs. (12.8 ^{14}C ka) (Darby et al., 2002). The 15.7 and 15.9 kyr ^{14}C age is close enough to Dyke's 16.2 ka to be the same event.

Ice Rafted Detritus and Ice Sheet Collapse

Conventionally, IRD is defined as sand-sized and coarser grains transported to open water by icebergs during times of increased calving and meltwater flux (Andrews, 2000.) Two types of IRD cycles are found in the North Atlantic, Heinrich (H) events and Bond Cycles. Bond cycles may be linked to the North Atlantic's 1-2 kyr climate cycle and correspond to Dansgaard/Øeschger cycles, first seen in the Greenland ice cores (Dansgaard et al., 1993). Bond layers are rich in sub-Arctic petrologic tracers (Icelandic glass and hematite-stained quartz) (Bond et al., 1999). H events (the timing of these are shown as blue bands in Figure 2) are IRD events characterized by low magnetic susceptibility, low grayscale levels, an increase in sand size detrital carbonates and lithics, and a decrease in planktonic foraminifers. H events occur at the end of Bond cycles and tend to have a rough cyclicity of ~7000 years (MacAyeal, 1993; Rashid et al., 2003). H events are purely North Atlantic phenomena involving IRD from the eastern portion of the Laurentide Ice Sheet and occur in a belt from 40°N to 55°N (Grousset et al., 1993). H events are connected to rapid climate change in the North Atlantic (Broecker, 1994), although the exact nature of this connection is still debated. There is some speculation that Arctic IRD events may be due to the same mechanisms as H events and may even involve similar volumes of glacial ice (Stokes et al., 2005). Precursors to H events consisting of IRD from smaller European ice sheets have been proposed (Fronval et al., 1995; Scourse et al., 2000; Grousset et al., 2000) suggesting that changes in the dynamics or collapse of small ice sheets, perhaps in response to climate change, may trigger changes in the LIS. The relationship between Arctic IRD and North Atlantic IRD cycles is not entirely clear. The Arctic IRD events seem to correspond to the timing of H events (Darby et al., 2002). This mismatch in timing could possibly be due to the vagaries of dating methods and criteria for when these events began. The largest problem in correlating North Atlantic Heinrich Events to IRD events in the Arctic is in dating Arctic materials. Additional problems can arise from variable definitions of Heinrich Layers. Some investigators define Heinrich Events only as coarse IRD peaks where others define them as carbonate rich IRD peaks (Bond et al., 1999). In this paper, Arctic IRD events are defined as peaks in Fe grains matched to specific ice sheets or peak abundances of lithic grains typical of specific ice sheet sources and Heinrich Events correspond to the definition proposed by Bond et al. (1999).

The mechanisms for producing IRD peaks in marine sediment cores are still being debated and include internal dynamics of ice sheets (MacAyeal, 1993), glacial growth on sensitive margins during periods of atmospheric cooling leading to increased calving during warmer periods (Bond and Lotti, 1995), the emptying of ice-dammed lakes (Johnson and Lauritzen, 1995), surges of ice streams (Marshall and Clarke, 1997), and catastrophic loss of a buttressing ice shelf (Hulbe et al., 2005). It has been proposed that small ice sheets may have a lead-lag relationship with the larger LIS that produced the Heinrich Events. This might occur due to a climatic or circulatory triggering that either is initially felt in the small ice sheets, or that instabilities in small ice sheets are transmitted to larger ones, perhaps by a sudden sea level rise caused by the surging small ice sheet (Grousset et al., 2000; Grousset et al., 2001; Darby et al., 2002).

CHAPTER II

METHODS

Study Area

Fram Strait is more than 3,000 km from the margins of the IIS and LIS, so only major IRD events should be present in the sediment record at this great distance. Due to ocean circulation patterns, Fram Strait is the only way for icebergs to exit the Arctic. A large volume of bergs passing through this area increases the chance of an event being preserved in the record. Three of the cores that were reexamined are from Fram Strait, but Fe grain data from only one of these (PS1230) has been published. Core 94BC28 is from the Lomonosov Ridge, an area that one would expect to receive some melt-out from both the Trans-Polar Drift (TPD) and Beaufort Gyre (BG), if both operated in a similar manner in the past as they do today (Figure 3). Other cores were used to correlate events across the Arctic, but did not undergo any added analysis. All cores used in this study are shown in Table 1.

Ice drift in the Arctic Ocean is influenced by the Beaufort Gyre, which brings ice in a clockwise motion from the QEI into the Beaufort Sea and eventually, after perhaps several rotations in the Gyre, northward to the central Arctic, where it joins the TPD, which transports ice from the Laptev, Barents, and Kara seas toward Fram Strait (Figure 3). There is some controversy over whether these two major circulation patterns behaved in the same way in the past. Using geochemical fingerprinting of IRD, Bischof and Darby (1997) proposed a weakening of the Beaufort Gyre during portions of glacial intervals, which would allow icebergs calved from ice covering the Queen Elizabeth Islands to take

Table 1. Core locations used in this study.

Core	Coordinates	Water depth (m)	Geographic Region	Core length (cm)	Added Analysis?
94BC28	88° 52.4', 140° 10.8'E	1990	Lomonosov Ridge	42.6	Yes
PS1230	78° 54'N, 4° 48'W	1235	Fram Strait	47.5	Yes
PS1231	78° 54.6'N, 3° 59.4'W	2012	Fram Strait	32	Yes
1894	75° 48.8'N, 8° 18'W	1975	Fram Strait	90	Yes
94BC20	83° 10.20' N, 174° 6.36' W	3100	Wrangel Basin	37.5	No
94BC08	78° 7.68'N, 173° 23.09' W	1031	Mendeleev Ridge	39.18	No
B15	75° 43.8' N, 160° 35.38' W	2135	Northwind Basin	37.5	No
P6	74° 15.33'N, 160° 35.38'W	580	Chukchi Borderland	158.5	No
P1/B3	73° 42.4'N, 162° 44.6' W	201	Chukchi Shelf near Northwind Ridge	409	No

a northerly path and exit the Arctic more directly via Fram Strait rather than following the Beaufort Gyre. Phillips and Grantz (2001) refuted this using the logarithmic decrease in the abundance of clasts from the entire OIS 2 interval collectively that are greater than 2 millimeters in diameter. The geographic distribution of the clasts suggests that the Beaufort Gyre had not weakened on average over this glacial interval. This controversy has not been resolved, but the recent findings of massive ice groundings on the Chukchi Borderland suggest that at some point during a large calving event, ice grounded there and probably diverted newly calved ice more northward into the central Arctic (Darby, personal communication 2006; Polyak et al., 2001; Polyak et al., 2007). The existence of grounded ice could easily resolve the controversy because the evidence used by Phillips and Grantz (2001) would not distinguish this interval of diversion from overall average BG circulation.

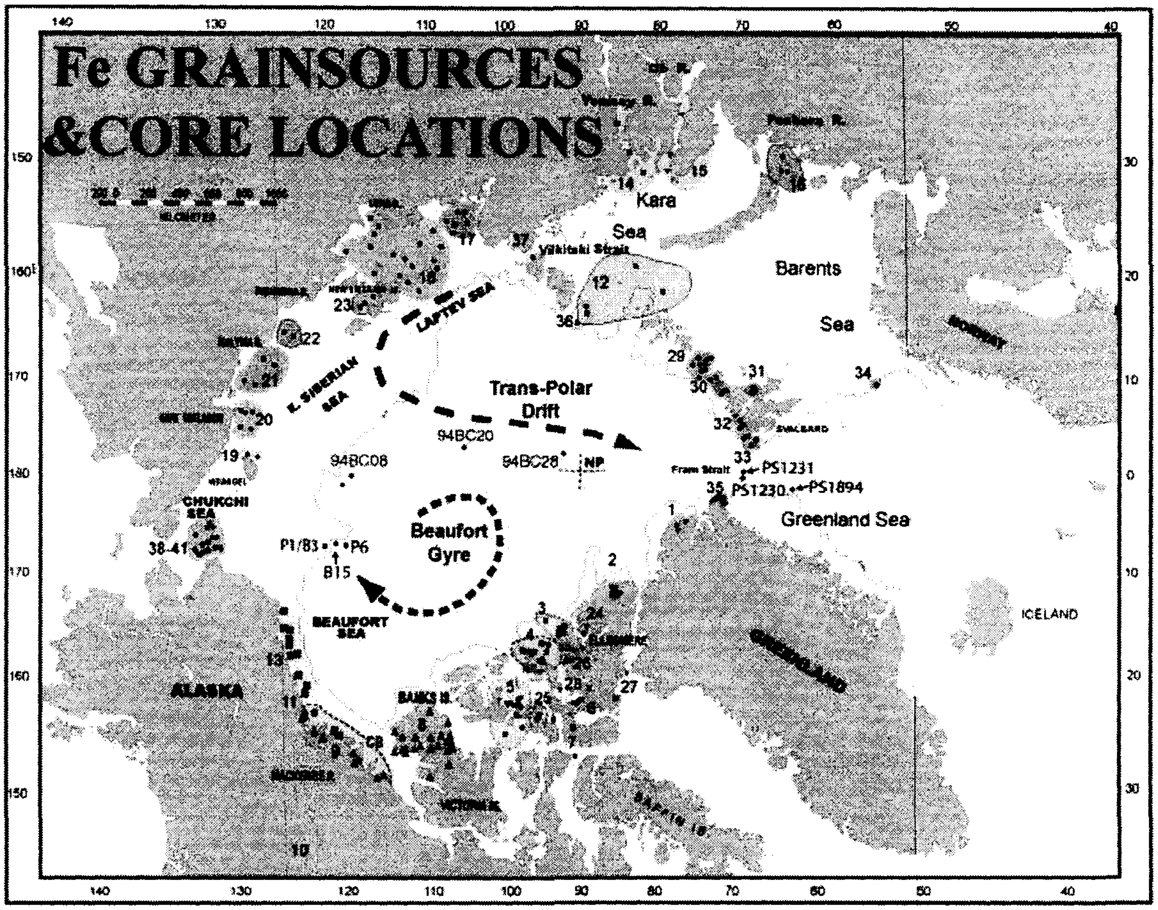

Figure 3. Location of sediment cores used and the circum-Arctic source areas along with the modern surface drift patterns (after Darby, 2003).

Analysis of Data

Geochemical fingerprinting can be used to match detrital iron oxide grains to Circum-Arctic source areas (Darby, 2003). Using this method, it is possible to determine which IRD came from the Innuitian and Laurentide Ice Sheets (Darby et al., 2002). It is also possible to determine from which characterized source area for a given ice sheet that an iceberg calved (Figure 3; Stokes et al., 2005). All sources from Siberia east of the Barents/Kara Sea are assumed to be from sea ice because no known glaciers calved into the Laptev or East Siberian Sea during the Wisconsinan (Figure 3). The same is probably true for the Chukchi Sea and Alaskan Arctic coast, but this is less certain. The known areas of glaciers on the circum-Arctic rim are the LIS (Banks Is.), IIS (all of the QEI), Northern Greenland, and the Barents Sea (Dyke et al., 2002; Brigham-Grette et al., 2003; Mangerud et al., 2002; Peltier, 1994).

The sharp peaks in the >63 and > 250 μm coarse fraction are used to determine the probable occurrence of major calving events. Sea ice transported grains are usually less than 100 microns. Grains up to cobble-size are possible, but very rare. It was assumed that peaks in the coarse fraction corresponded to a greater number of glacial bergs being produced (Andrews, 2000) and would therefore serve as a rough guide to times of increased calving. Additional grains at each interval of each IRD peak were analyzed using the Fe grain fingerprinting method (Darby and Bischof 1996). The new data was combined with previous results (Darby et al., 2002) to give a clearer picture of source areas at the peaks and the relative abundances of Fe grains matched to either the IIS or LIS. The signals are much clearer after additional analysis (Figure 4).

In order to avoid misleading peaks due to low numbers of matched grains in some intervals, a weighted percent for each source area at each depth was determined by multiplying the number of grains matched to a given source area at a given depth by the percentage of these matched grains at that depth and dividing by 10 (Darby, 2003). Thus if there were ten grains matched to a source, the weighted percent and normal percent are the same. Fewer grains would reduce the weighted percent and more than 10 would increase the weighted percent over the normal percent. Ten grains matched to a source is

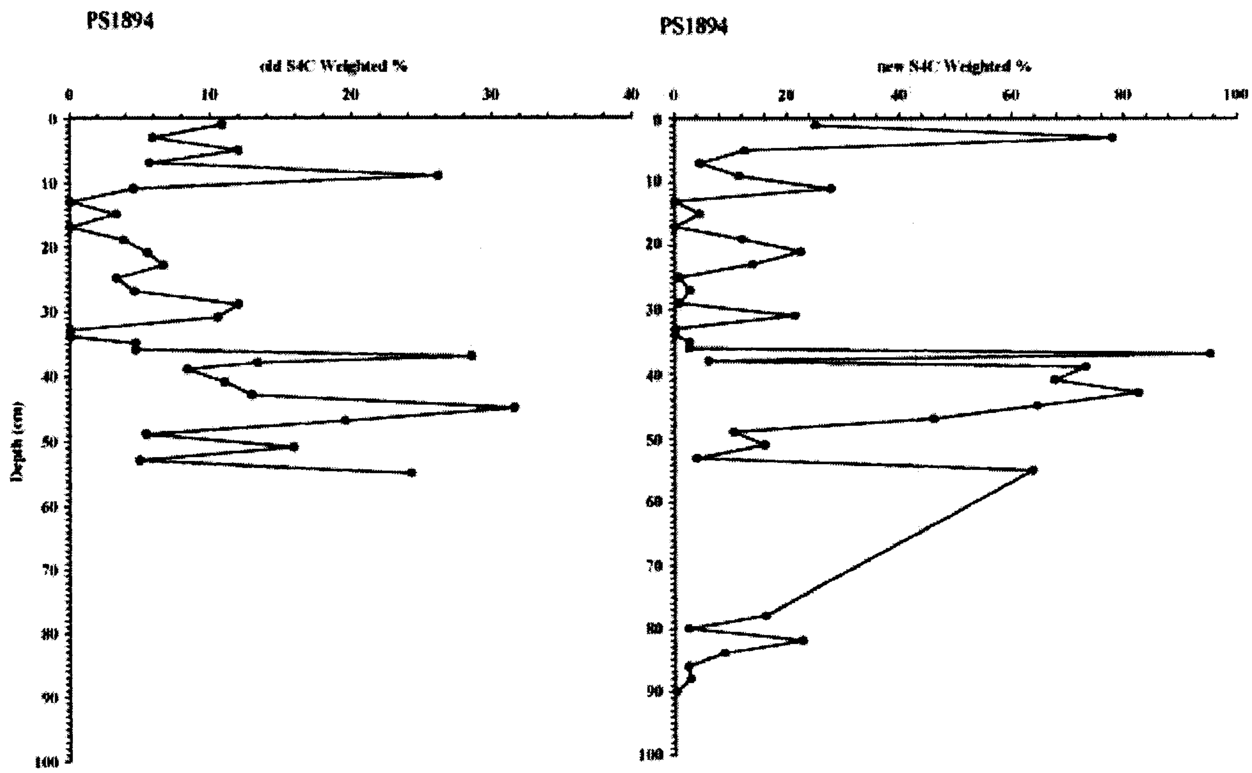

Figure 4. Comparison of previous and new data for the combined source areas of Banks Island (S4C) in core PS1894. While Fe grain peaks matched to Banks Island are generally still present at the same depths, their shape has changed with the additional analyses. The dramatic slope between the data points at 55 cm and 75 cm are due to a lack of data in that interval.

a critical threshold because in a test of this matching technique less than eight to ten grains matched to sources that were from outside the Arctic and thus are impossible sources of Arctic sediment (Darby, 2003).

Plotting Data and Picking Peaks

Weighted percents of Fe grains from the combined Innuitian area (source area 4C, all of the northern QEI sources, which includes source areas 2, 3, 4, 24, and 26 on Figure 3) and Laurentide area (source area 8, Banks Island) are plotted for each of the cores versus depth and time. Taking a three-point average of the weighted percents further smoothed the data. Using this average avoids misleading peaks and lows caused by spurious points and low grain numbers in a few samples.

Icebergs containing Fe grains matched to source 8 were most likely calved from the M'Clure Strait Ice Stream (Stokes et al., 2005). The main northward flowing IIS ice stream was in Massey Sound between Axel Heiberg and Ellef Ringnes Islands in the QEI (England et al., 2006). The Fe grains matched to the shelf source area near Ellef Ringnes Island are commonly the most frequent source for Fe grain peaks matched to the IIS source. Background levels of weighted percent in this paper are defined as 8%, which is considered the minimum for being significant based on tests with several thousand Fe grains from the Arctic matched to source groups along the eastern U.S. coast (Darby, 2003).

Peak centers (average age or depth of peaks in each core) are picked graphically. Peaks are defined as portions of the graph where the weighted percent, 3 point running average, is much greater than background. The maximum weighted percent of the peak is multiplied by 0.75 to get a 3/4-peak height. A line perpendicular to the X-axis is drawn at the 3/4-peak height, which intersects the two limbs of the peak. (If the line does not intersect a limb, the limb is extended until it intersects the line.) The peak center is the midpoint of the line intersecting the peak limbs.

Other Sources of Error

There are several issues of concern when working with sediments from the Arctic Ocean. First is the generally low sedimentation rate during glacial cycles when thick pack ice and ice shelves are present. The low sedimentation rates of glacial conditions are usually followed by a surge of IRD marking deglacial conditions that cause high sedimentation rates for a brief period. Moderate sedimentation rates occur during interglacial intervals, lower than during deglacial events, but higher than full glacial intervals. Interglacials typically last longer than deglacial events and thus are represented by thicker deposits. Sedimentation rates on the central Arctic Ocean ridges can vary from less than 0.5cm/kyr during glacial times to over 1-2 cm/kyr during interglacials and over 5 cm/kyr during deglacial events (Darby et al., 1997; 2002). A change in freshwater circulation and ventilation also affects productivity, leading to differences in the amount of biogenic remains (Polyak et al., 2003). There is some controversy over average sedimentation rates in the central Arctic Ocean (Jakobsson et al., 2003; 2000). The Eurasia basin appears to have average sedimentation rates of 1-2 cm/kyr, while the Amerasian basin has a 1-2 mm/kyr rate (Clark et al., 1980; Darby et al., 1989) except in the Holocene where rates of about 1 cm/kyr were found (Darby et al., 1997). This issue of average sedimentation rates being different by an order of magnitude will hopefully be resolved with the age dating effort currently underway on the new Healy-Oden Trans-Arctic Expedition cores (Darby et al., 2005). Backman et al. (2003) suggested that these apparently different rates of sedimentation are due to inaccurate age modeling. This brings up the second complication to be considered when working with Arctic Ocean cores, age models for cores.

One of the biggest potential sources of error for radiocarbon dates on marine sediments is the reservoir correction, which can vary from 400 years (North Atlantic value) to around 1000 years for higher latitudes (Beck et al., 2001; Robinson et al., 2005). Reservoir corrections account for the differences in the age of carbon dissolved in deep waters in different oceans. Upwelling of this deep, older water brings it towards the surface where carbonate secreting organisms utilize it. Old carbon can reside in the deep ocean for hundreds to thousands of years until it is brought to the surface. Unless this is accounted for, an incorrect date will be calculated (Stuiver et al., 1986). A too-large ^{14}C reservoir correction will yield a young age and a higher sedimentation rate (Backman et al., 2003). A correction of 740 years for suspension feeding mollusks in the Canadian Arctic Ocean has been suggested based on pre-bomb mollusk shells that were collected alive and later tested for radiocarbon age (Dyke et al., 2003). This high reservoir factor is probably due to some old carbon eroded from limestones into the coastal waters in the Canadian Arctic. This correction has not been used by all workers and in papers published before 2003 estimates for the reservoir correction has ranged from 300 years (Blake, 1992) to the standard oceanic average of 400 years used by the Calib 5 program. Yet another source of error occurs in how the age model is interpolated between dates. (Andrews et al., 1999).

While errors in dating make it difficult to correlate cores, changes in the Laurentide and Innuitian signals can be compared in the same core regardless of absolute age. Distances between peaks can be interpreted as separations in time, even though the exact duration of time each separation represents is unknown. For instance, an IIS event that occurs two centimeters downcore from an LIS event can be said to have occurred before the LIS event, even though it is uncertain how much time elapsed between the two events. In this paper, depth versus age plots are constructed using data from Calib 5.0 for all ages younger than 15 radiocarbon ka and the Fairbanks model for all ages 15 radiocarbon ka or greater. Two separate age models were used due to the limitations of the Calib 5.0 dataset. The Fairbanks model can be used for dates extending back to 50 kyr. The Fairbanks model is available online at http://www.radiocarbon.ldeo.columbia.edu. The 440 year correction (Bauch et al., 2001) will be used for both the Fairbanks model and Calib 5.0 in the interest of comparison with other works. The number of radiocarbon dates per core undergoing additional analysis is shown in Table 2:

Table 2. Number of radiocarbon dates for cores undergoing additional analysis.

1894	94BC28	1230
7	8	12

CHAPTER III

RESULTS AND DISCUSSION

Innuitian Conditions

The extent of the IIS during OIS-2 and whether bergs calved only from ice streams established in specific fiords were two questions considered in this study. Plots of the change in weighted percentages of materials coming from the five different source areas of Ellesmere Island (Figure 5) in PS1230 suggest that the IIS shed bergs mainly from source area 4. The peaks of individual Ellesmere source areas seen in a core may be due more to physiographic causes such as the size of calved icebergs and whether they had a deep enough draft to contact warmer water at depths in excess of 300 m (North Atlantic Intermediate Water) and thus affect melt rate.

There appears to be some IRD transport by glacial or sea ice for most individual IIS source area (These are grouped into combined source areas when comparing the IIS to the LIS) during calving events. Massey Sound appears to have been the dominant ice stream throughout the Wisconsinan. This is consistent with the findings of England et al., 2006).

The production of ferromagnetic grains from the Siberian sources believed to be unglaciated appears to have occurred throughout the Wisconsinan. Grains matched to unglaciated Siberian sources are present in all cores. The majority of the grains come from the Laptev Sea (Figures 22-25; Appendix A, Figure 3). The sea ice signal drops below significance at 27-33 cm depth in PS1230, 3-6 cm depth in PS1231, above 10 cm in 94BC28, and is hovering near significance for almost all of 1894. The weighted

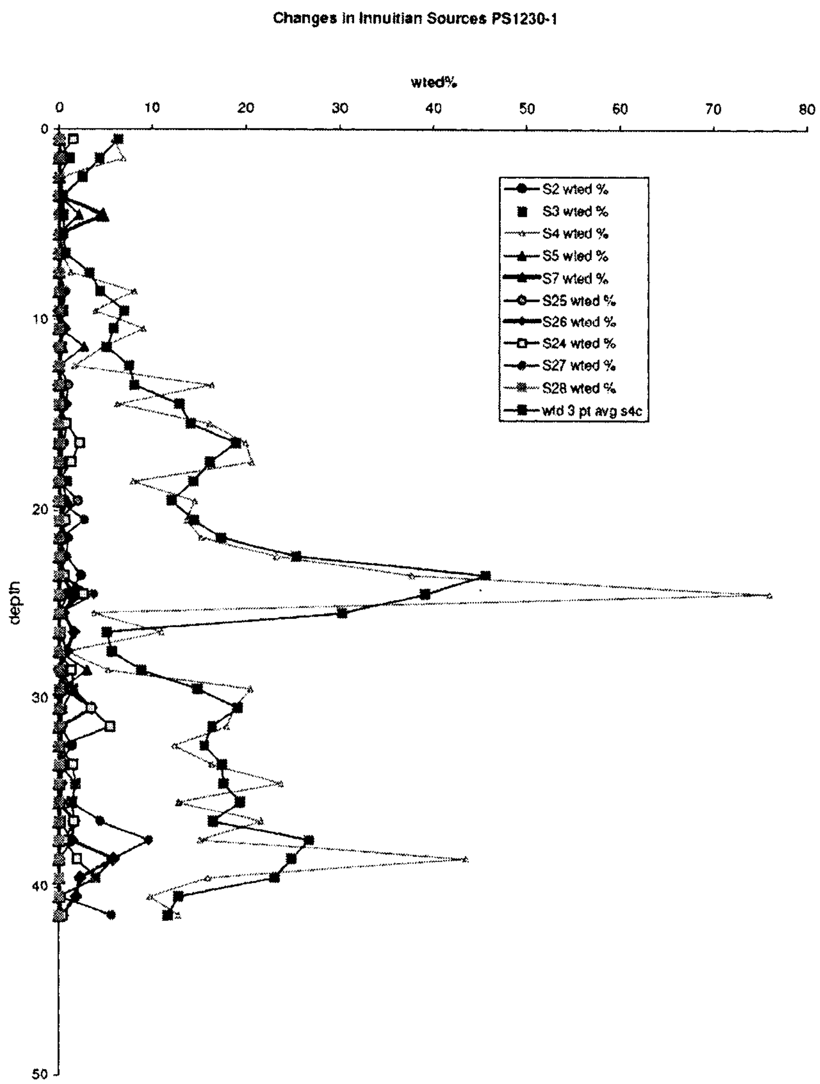

Figure 5. Fe grain peaks from all Innuitian grains sourced to Ellesmere Island. Note the majority of Fe grains come from Massey Sound (S4).

percent of Fe grains matched to unglaciated sources of sea ice production was plotted alongside the weighted percent of Fe grains matched to an ice sheet source area for each core (Appendix A). When the amount of Fe grains matched to glaciated areas was high, the amount of Fe grains rafted solely by sea ice was less abundant. Conversely, when many Fe grains could be matched to areas of sea ice entrainment, there were few Fe grains matched to the areas covered by ice sheets. The two were never equally abundant or abundant at the same time. This pattern could be showing that the sea ice signal was being drowned by the amount of grains melting out of glacial bergs during deglaciation, or it could be a problem with closure when only a few sources contribute to a sample.

Calving events from glaciated areas that do not occur near peaks in the coarse fraction may be more appropriate for reflecting changes in sea ice transport, as coarse grains are generally transported by glacial bergs as opposed to sea ice. An example of this is the LIS peak in Figure 10 around 2 cm. As both glacial bergs and sea ice can come from some of the same source areas, the signals cannot be readily separated by the methods used in this study.

Analysis of the data shows five correlatable collapse events in the Fram Strait cores (Figure 6). These generally correspond to the average times of Heinrich Events in the North Atlantic, i.e., 12.2, 15.5, 23.3, and 31.6 cal. ka. The Fram Strait cores show collapse events at 11, 15, 18, 22.9, and 25.9 cal. ka. The Arctic events at 18 ka and 26 ka do not seem to have a Heinrich equivalent. In these cores, it appears that the Arctic collapse events either lag or correspond to Heinrich Events. Events 2, 3, and 5 are the largest Arctic IRD events and each of these events is represented by a sharp rise in the volume of Fe grains matched to both the IIS and the LIS. This sharp rise in volume is used to suggest a rapid influx of glacial bergs from IIS and LIS sources (Darby et al., 2002). A similar rise in Fe grain volume from LIS and IIS sources is seen in the Holocene of cores 1894 and 1231. This Holocene rise likely represents a rapid influx of sea ice IRD from source areas once covered by the IIS and LIS. The lack of IRD event 1 in 92BC17 (Figure 7) may be due to the grounding of ice on the Chukchi area diverting bergs to the north around the core site.

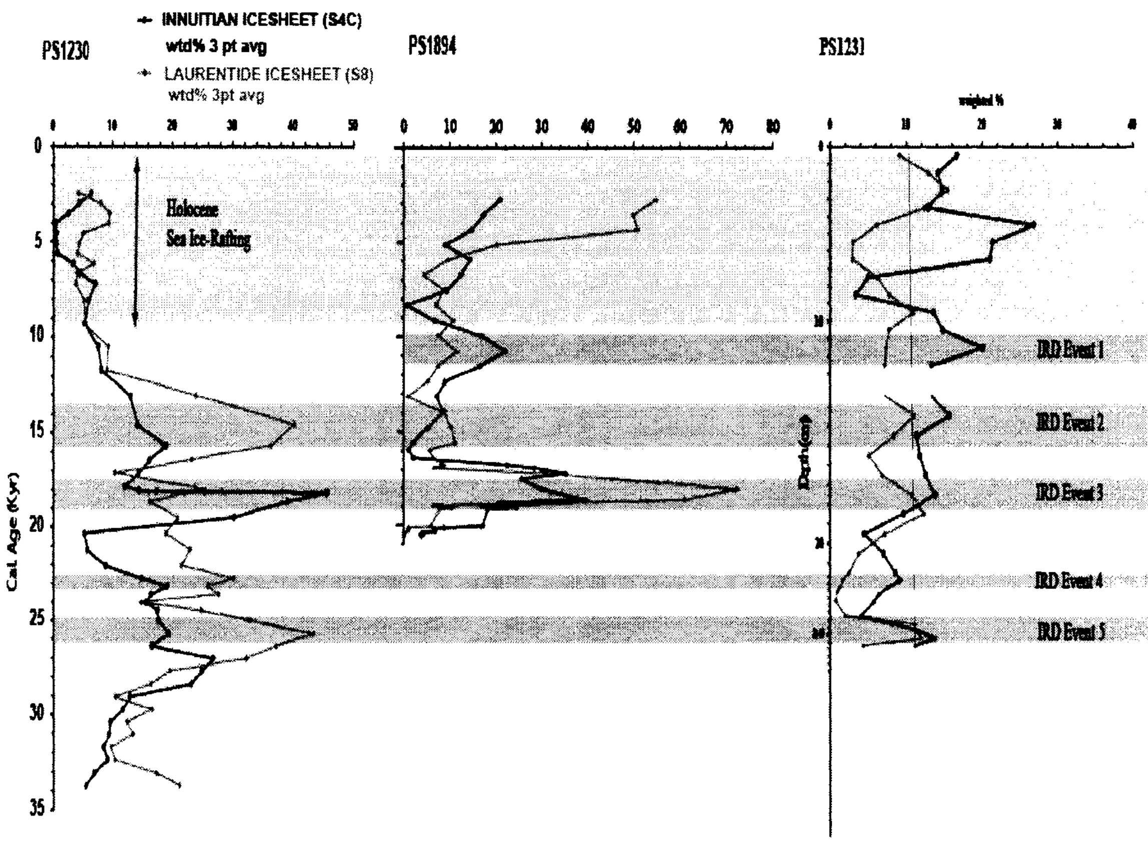

Figure 6. Correlation of collapse events in Fram Strait Cores. IRD Event 1 is not seen in PS1230.

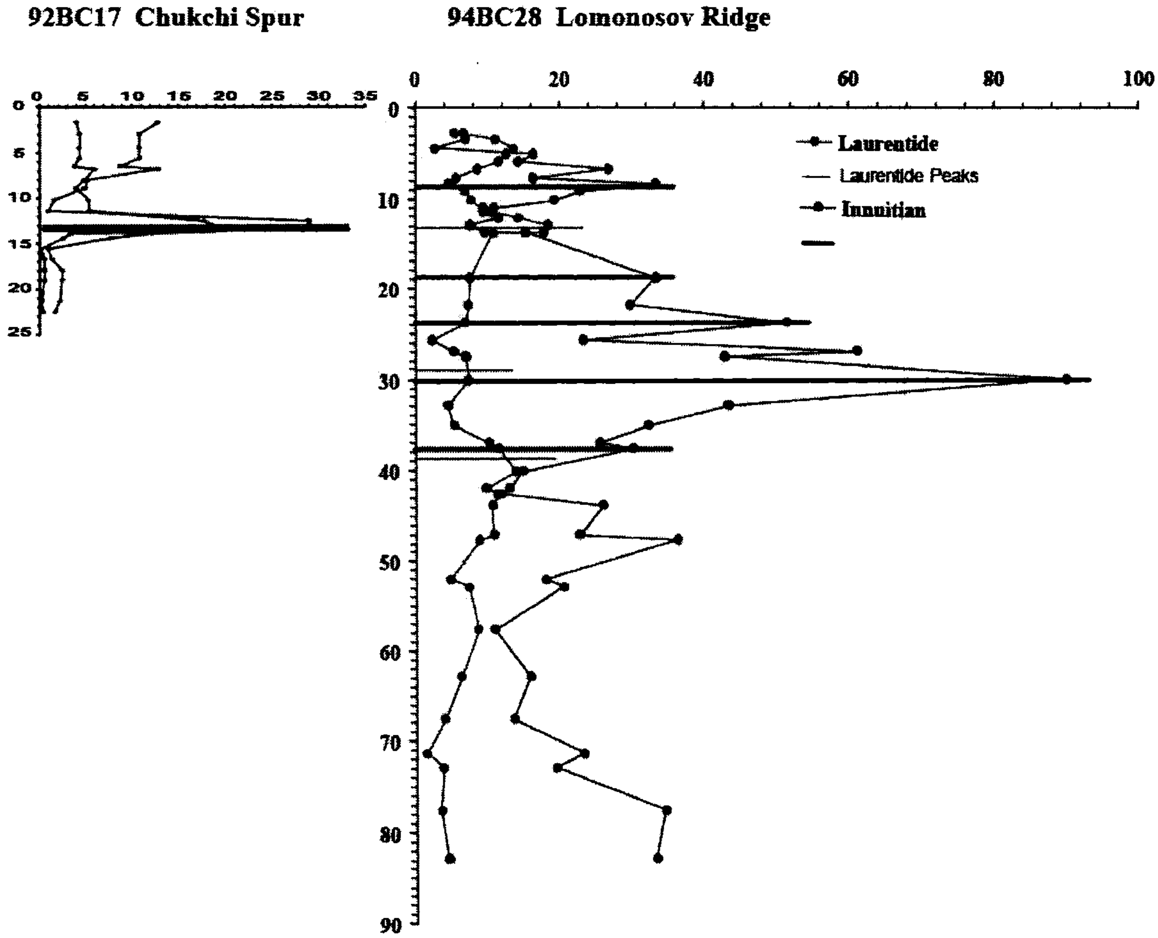

Figure 7. Correlation of collapse events in the Chukchi Spur and Lomonosov Ridge. Deposition in the Chukchi Spur may have been influenced by grounded ice. All dates below 45 ka are speculative.

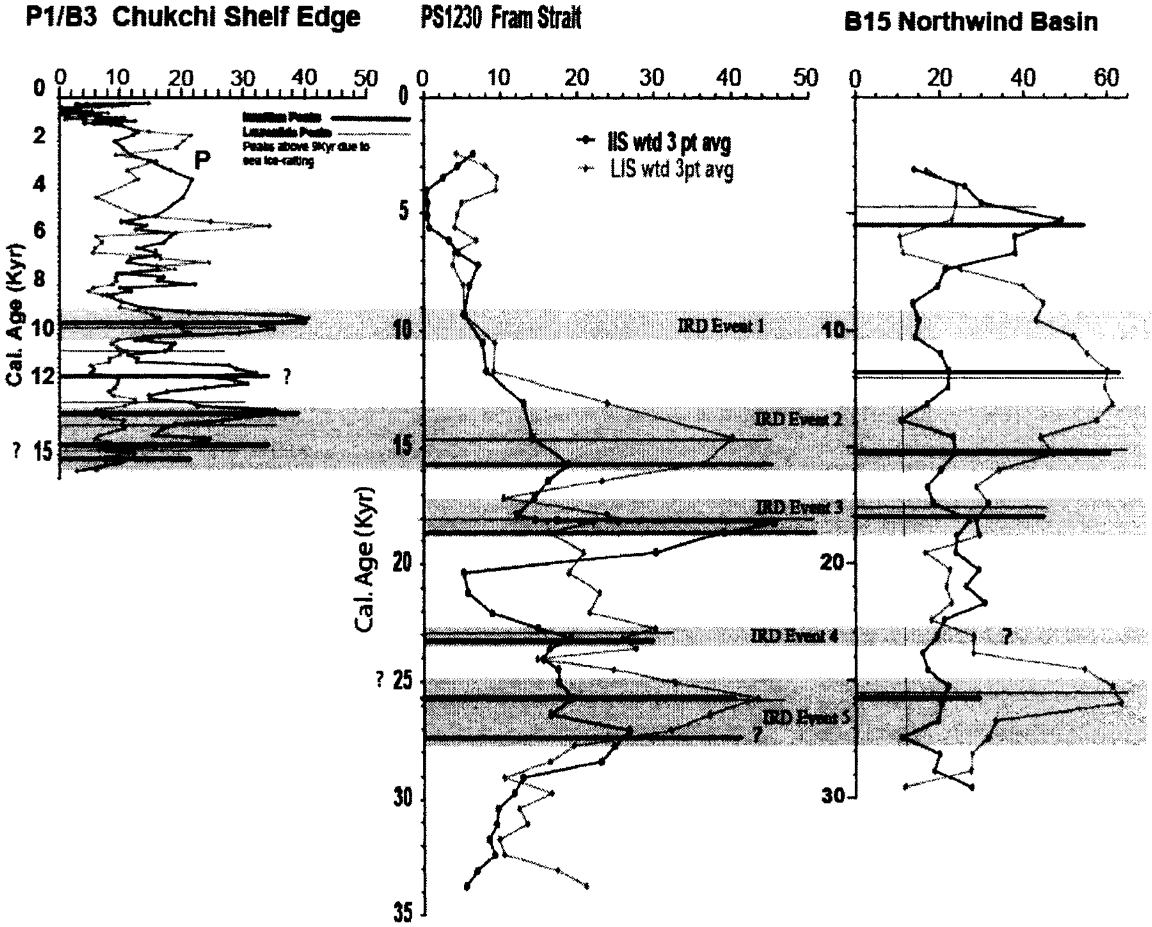

Figure 8. Correlation of collapse events in the Chukchi Shelf Edge, Fram Strait, and Northwind Basin. Both the Chukchi Shelf and Northwind Basin show an IRD event around 12ka not recorded in the Fram core. Ages older than 8ka in core P1/B3 are speculative.

Is There a Lead-Lag Relationship between IIS and LIS?

More dates were taken on core PS1230 than any other core reanalyzed, giving it the best age control. Four definite IIS peaks and five definite LIS peaks are seen in PS1230 (Figure 9; Figure 10). There is possibly another peak for each ice sheet, but these peaks are below background and may be insignificant. The lead-lag relationship is less clear in the reanalysis of PS1230 than it appeared in Darby et al., 2002. Using the proximity of one event to another it could be argued that the LIS is leading the IIS with a long lag time or the IIS is leading the LIS with a short lag time. However, when the portion of the core with the highest resolution and best age control is considered (at 18 ka), there is a clear IIS lead of only a few hundred years or less to the LIS collapse event recorded in this interval (Figure 6 in Darby et al., 2002).

There are two events in PS1230 that are only represented by one ice sheet and two events below significance . The two events below significance are at 9 ka (IIS) and 7 ka (LIS). Unpaired events occur throughout the reanalyzed cores. These "lone events" [where an event from one ice sheet does not correspond to an event from the other ice sheet] could be due to: a) a truly lone event, i.e. collapse of just one ice sheet and not the other, b) poor preservation of the partner event, c) how the core was sampled, or d) less melt-out of larger LIS bergs in Fram Strait (for lone IIS events). There is an LIS event at 30.5 ka with no corresponding IIS event because the core ends at this point.

Closure does not appear to be much of a problem in PS1230 as the IIS 3-point weighted percents are not at a minimum when LIS 3-point weighted percents are at a maximum, and vice versa. Since there is no problem with closure, the highs and lows in Fe grain volume are real, and not an artifact of the smoothing process. Source area peaks are often within a few centimeters of coarse fraction peaks, but do not typically occur at the same time as a peak in the coarse fraction from all source areas. All events are between 2 kyr and 1.5 kyr in duration.

Both PS1230 and PS1231 were taken in the vicinity of 78°51'N 04°46'W, and should theoretically show similar trends in ice sheet collapse due to their close proximity

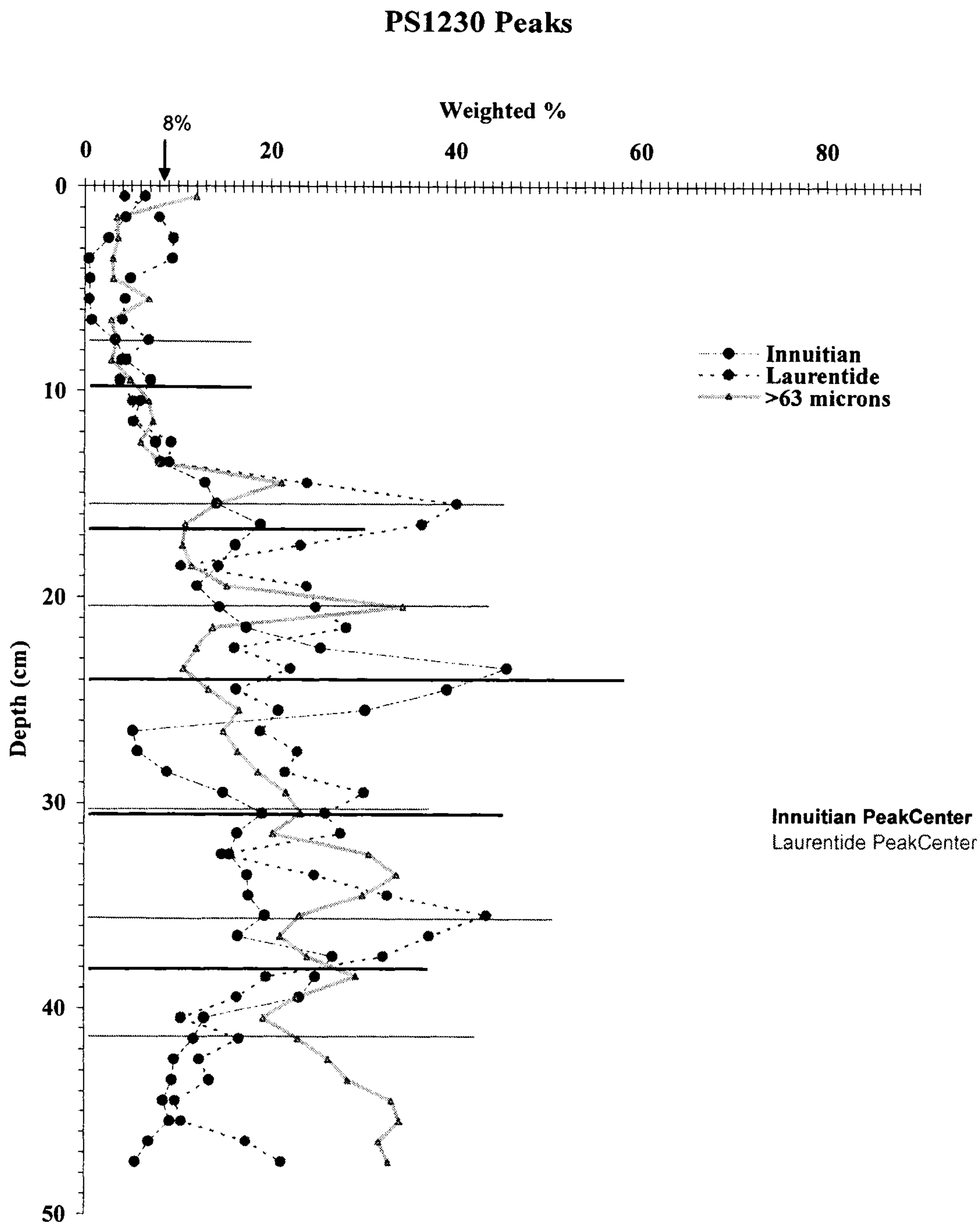

Figure 9. Comparison of weighted percent of Fe grains matched to Innuitian and Laurentide sources in core PS1230 from Fram Strait. Coarse fraction is also shown. Note Fe grain peaks do not necessarily coincide with coarse-grained IRD events. Depth is cm below sea floor.

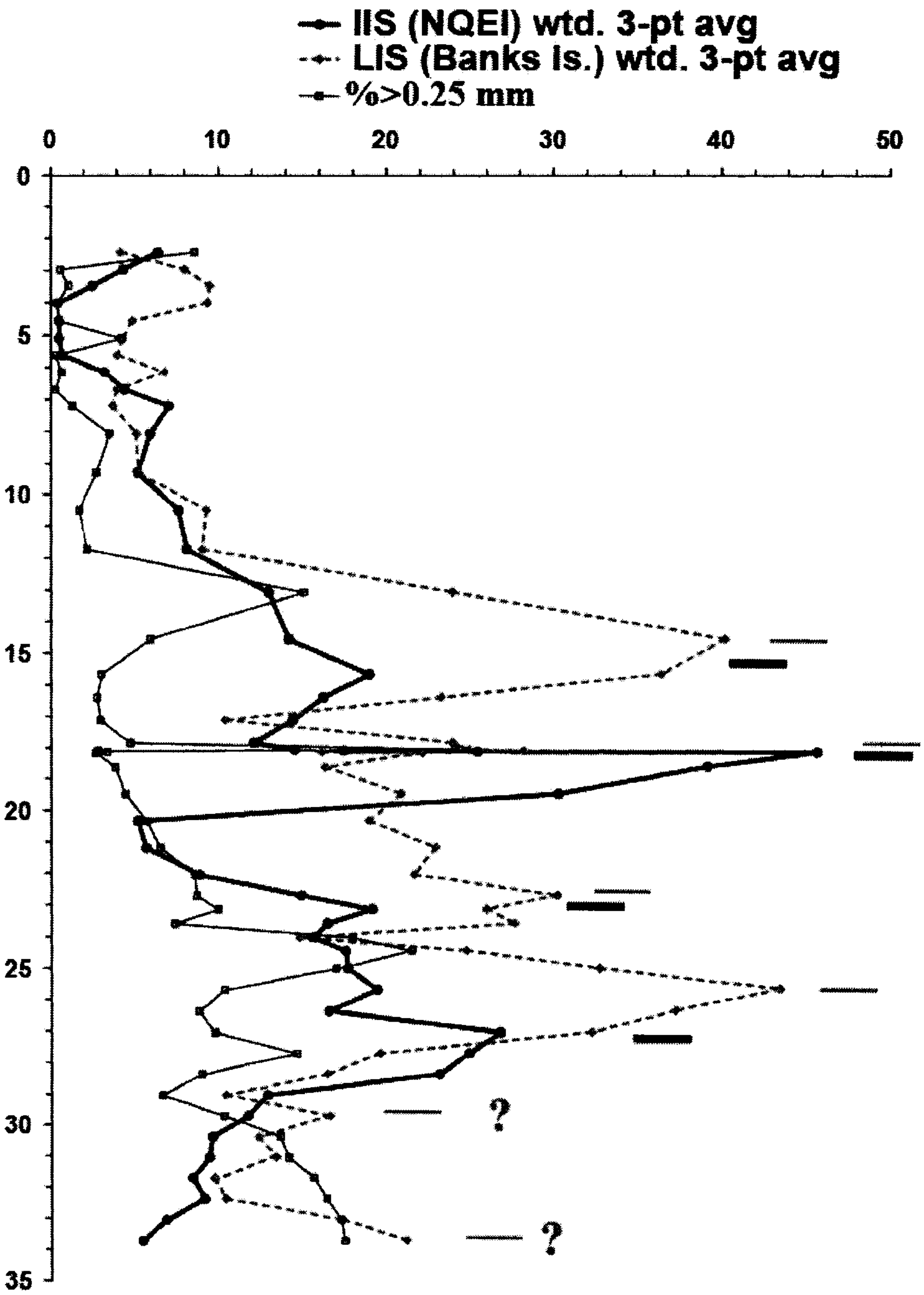

Figure 10. Fe grain weighted percents matched to the LIS and IIS in PS1230. The age control is best for the period of rapid sedimentation near 18 ka. The two events near this time have the closest spacing, around 250 years. See Table 3 for ages of peak centers.

Table 3. Summary of matched Fe grain peaks in core PS1230. dbsf = depth below sea floor. As a check of the age model, two methods were used to determine the date of peak centers. The peak center determined graphically was found by using the age vs. weighted % graph. Peak center calculated from age model is the date given by the age model for the ¾ peak center in cm. The difference in Ka is the absolute value of the peak center calculated from age model subtracted by the peak center determined graphically. This value can be used as an accuracy check to see how well the age model predicts where a peak will occur. In PS1230, the differences are small, which one would expect in a core with good age control.

	depth vs. weighted %			age vs. weighted%		
IIS	3/4 peak center, cm (dbsf)	peak width in cm	Peak center calculated from age model	Peak center determined graphically	Difference in Ka	Duration in Kyrs
	16.75	2.75 cm	15.71	15.5	0.21	2
	24	2.25cm	18.81	18.25	0.56	1.5
	30.75	2.25 cm	23.04	23.2	0.16	1.75
	38.25	3 cm	27.73	27.5	0.23	2
LIS						
	3/4 peak center, cm dbsf	Peak width in cm	Peak center calculated from age model	Peak center determined graphically	Difference in Ka	Duration in Kyrs
	15.5	2.5	14.48	14.5	0.02	2
	20.5	2.9	18.04	18	.04	2
	30.25	3.25	22.73	22.5	0.23	2
	35.75	3	26.17	25.5	0.67	1.9

to one another. Random events, such as where an iceberg from a given source area happened to melt, can produce more matches to that source area in one core than another. As expected, PS1230 and PS1231 show the same general pattern but contain some differences. The differences between the cores could result from the core depth and the methods used for dating as well as from random events. PS1231 (Figure 11; Figure 12) is shorter than PS1230 and the age model for PS1231 was constructed using radiocarbon dates from PS1230 due to their close proximity. The cores were correlated using peaks in the coarse fraction (>250 μm) in order to transfer the age model.

Because PS1231 is fairly close to PS1230, it should help confirm the patterns seen in PS1230. The IIS in PS1231 appears to be leading the pairs of peaks around 24 ka and 4 ka. There appears to be a very slight IIS lead of the pair of peaks at 13.5, but the lead is so slight that these events can be considered to have occurred simultaneously. The LIS leads the pair of peaks around 15.5 ka. There is an LIS peak at 8.1 ka and at 13.5 ka, which could represent the final purging of the Laurentide Ice Sheet through M'Cure Strait. Land evidence points to the final ice collapse closer to 10 ka (Stokes et al., 2005). Thus the age model for this core, which is transferred from the nearby PS1230 core, could be slightly off. The IIS peak at 11.25 ka is closest to this McClure Strait event in time. All of these peaks and the dual IIS and LIS peak at 13.5 ka are missing in the PS1230 core. The LIS leads the IIS only at the 15 ka event, but there is an opposite juxtaposition of these two peaks in the PS1230 core at the same age (Figure 10). This reverse in leads between the two cores could indicate that the sampling intervals have a significant effect on the position of Fe grain peaks from these two sources. There is a lone IIS event at 17.5 ka that probably corresponds to the dual IIS and LIS peaks at 18 ka in PS1230. PS1231 peaks for the IIS and LIS are similar to PS1230 peaks at about 25 ka.

Because the IIS and LIS curves are not inverted from one another, closure does not appear to be a problem between LIS and IIS peaks so it can be discounted. Fe grain peaks do not necessarily correspond to peaks in the coarse fraction. Differences between calculated peak centers and graphically determined peak centers on the age graph are slight. All events are between 3 and 1.75 ka in duration. Peak centers, width, and

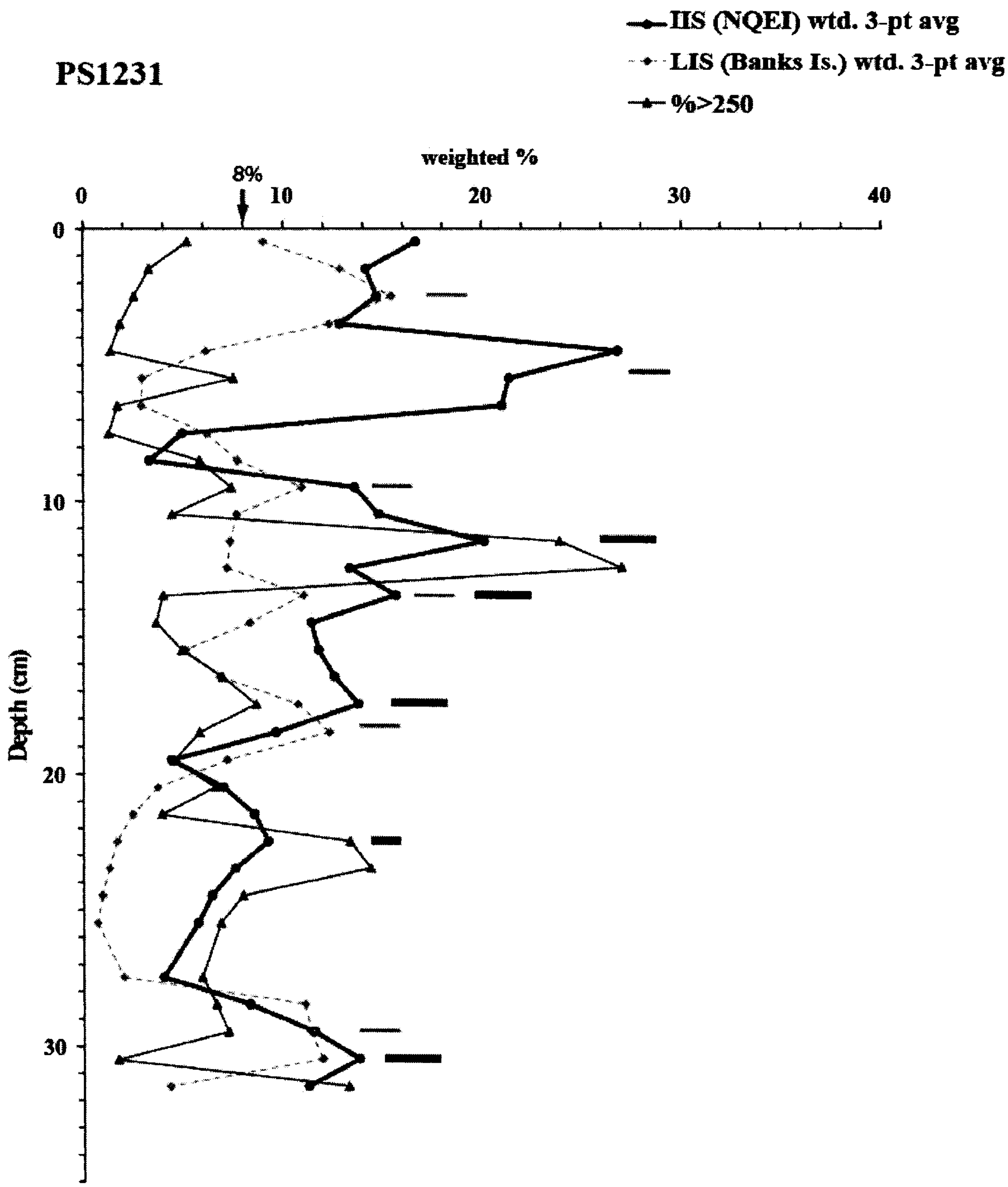

Figure 11. Comparison of weighted percent of Fe grains matched to Innuitian and Laurentide sources in core PS1231 from Fram Strait. Coarse fraction is also shown.

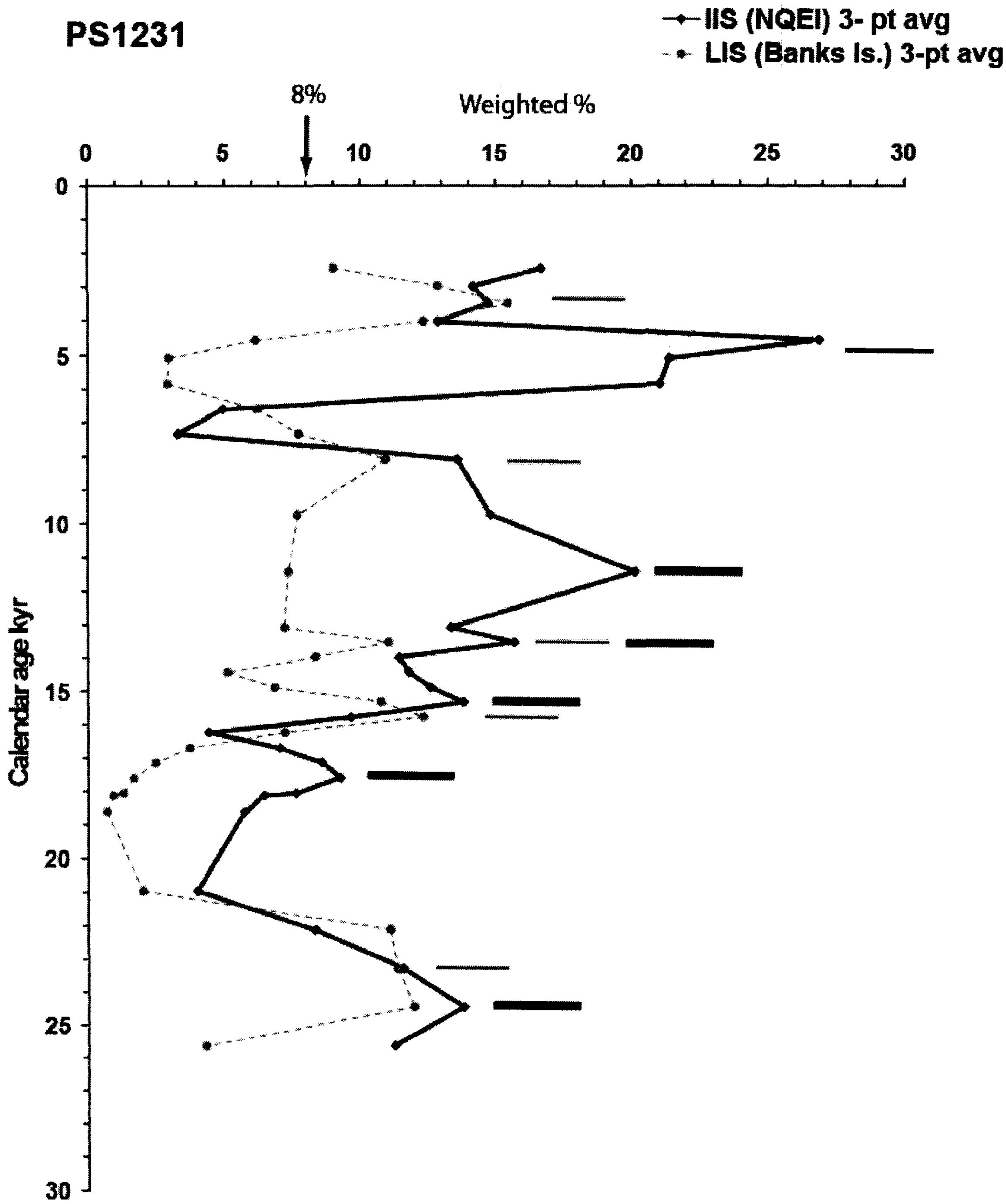

Figure 12. Changes in Fe grain weighted percent plotted against radiocarbon calendar age in the LIS and IIS, PS1231.

approximate lag time between LIS and IIS peaks are summarized in Table 4.

Core PS1894 (Figure 13; Figure 14) was sampled at 2 cm intervals instead of 1 cm, which decreases the resolution. It is also taken from much deeper water than the preceding two cores and might be influenced by different currents or have mixing/ventilation issues that would affect the radiocarbon dates separate from the other two Fram Strait cores.

As in core PS1230, the Fe grain peaks matched to the IIS and LIS do not correspond to peaks in the percent > 63 microns (Figure 13). This is probably due to the low melt out rates at these core sites, which are well north of the pack ice margin at this time. Instead, the increasing number of bergs from the ice collapses led to the increases in Fe grains matched to these ice sheets simply because small amounts of material melted from this larger number of bergs along the entire drift path and not massive melting of the berg once they reached open water. Sedimentation rates are fairly linear during all calving events (Figure 15). There is clearly a IIS peak prior to the LIS peak around 18 ka. with lag time of about 500 years (Figure 14). This is very similar to the situation in core PS1230 where four radiocarbon dates between 18 and 18.3 ka bracketing these peaks show an even shorter lag time of about 250 years (Figure 12; Darby et al., 2002).

The paired IIS and LIS event at 10.8 ka in PS1894 might be the M'Clure Strait Ice Stream Surge of ~10 ka (Stokes et al., 2005). Closure does not appear to be a problem because the minimum 3-pt average of one ice sheet does not occur at the same depth or time as the maximum 3-pt average of the other ice sheet. Differences between the graphically determined and calculated peak centers for the age vs. weighted percent plots are negligible. Fe-grain peak events range from 500 years to 1.75 ka in duration

Table 4. Summary of Fe grain peaks matched to LIS and IIS source areas in core PS1231.

Depth vs. wt %			Age vs. wtd %			
IIS	3/4 peak center cm dbsf	peak width in cm	Peak center calculated from age model	Peak center determined graphically	Difference in Ka	Duration in kyrs
	5.25	2.75	4.96	5	0.04	1.75
	11.5	2	11.42	11.25	0.17	3
	13.25	1.5	13.42	13.5	0.6	1.5
	18.25	3	15.69	15.25	0.44	1.5
	22.5	3	17.62	17.5	0.08	1.5
	30.5	1.75	24.48	24.5	0.02	3.5
Depth v. wt %			Age v. wtd %			
LIS	3/4 pk ctr cm dbsf	peak width in cm	Peak center calculated from age model	Peak center determined graphically	Difference in Ka	Duration in kyrs
	2.5	2.75	3.48	3.25	0.26	1 ka
	9.5	2	8.09	8	0.09	2 ka
	13.25	1.75	13.42	13.25	0.17	0.5 ka
	18.25	2	15.41	15.75	0.34	0.25 ka
	29.5	3	23.31	23.25	0.06	3 ka

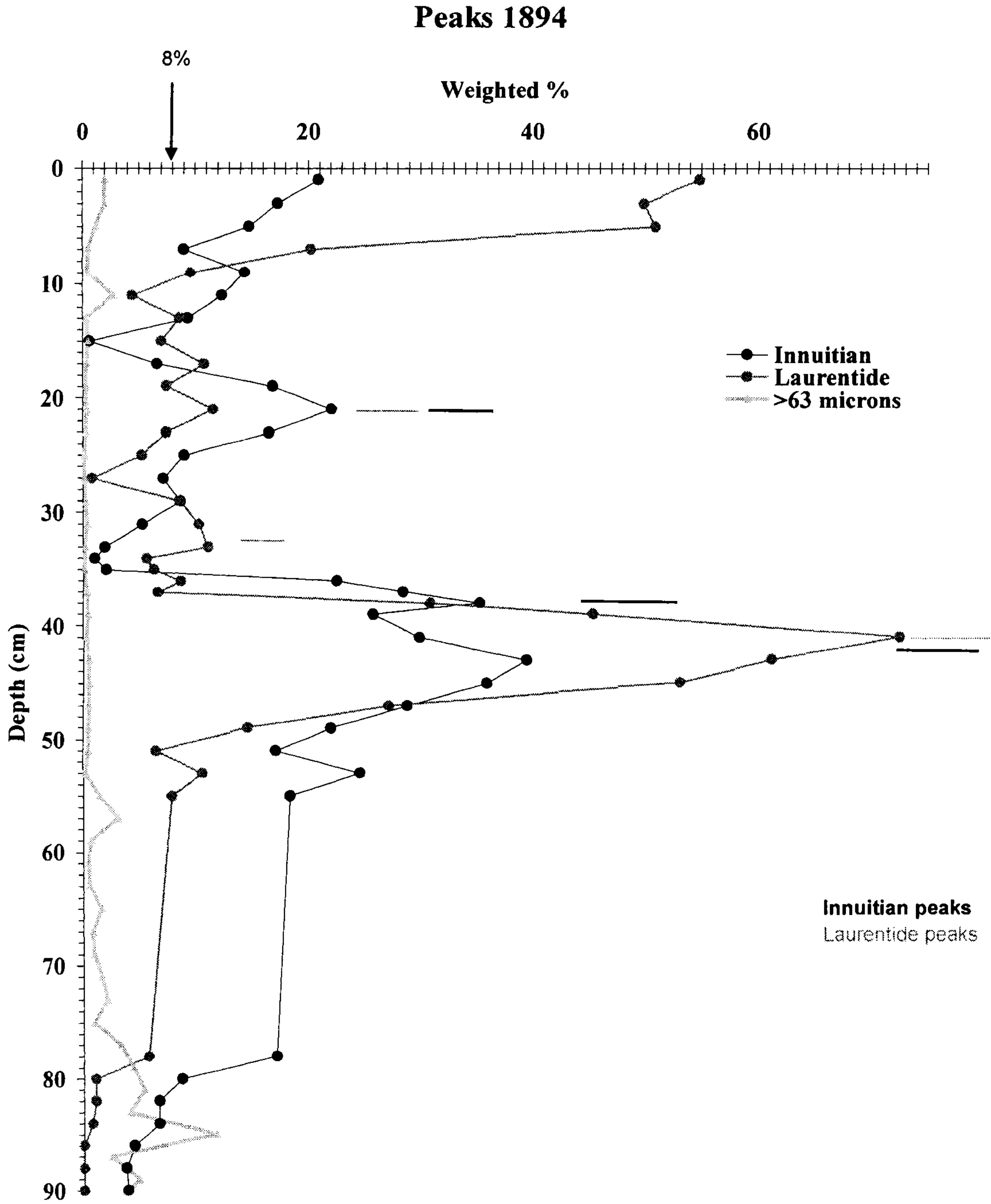

Figure 13. Comparison of weighted percent of Fe grains matched to Innuitian and Laurentide sources in core 1894 from Fram Strait. Coarse fraction is also shown.

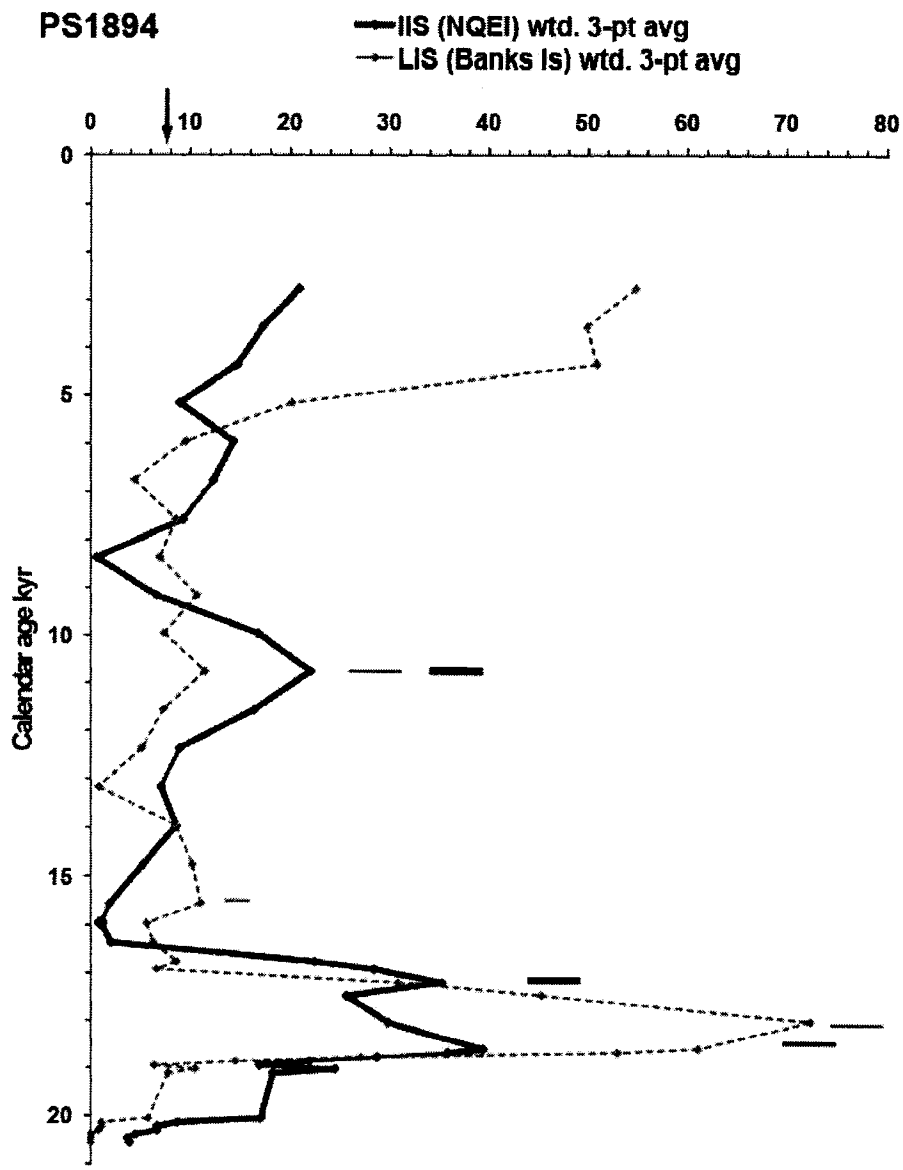

Figure 14. Changes in Fe grain weighted percent plotted against radiocarbon calendar years in the LIS and IIS, 1894. Note the close correlation of the large peak around 18 ka with the peak at 18 ka in core PS1230.

Table 5. Summary of Fe grain Fe grain peaks matched to LIS and IIS source areas in core PS1894.

depth v. wt %				age v. wtd %		
IIS	3/4 peak center cm dbsf	peak width in cm	Peak center calculated from age model	Peak center determined graphically	Difference in Ka	Duration in kyrs
	21.25	4	10.86	10.8	0.06	1.75
	38	2	17.56	17.2	0.36	1
	42	3	19.16	18.75	0.41	1
depth v. wt %			age v. wtd %			
LIS	3/4 peak center cm dbsf	peak width in cm	Peak center calculated from age model	Peak center determined graphically	Difference in Ka	Duration in kyrs
	21.25	2.5	10.86	10.8	0.06	1.5
	32	3	15.16	15.5	0.34	.5
	41.25	4	18.86	18.2	0.66	1

(Table 5).

The IIS signal is higher than the LIS, showing greater values in the weighted % of grains, until around 18 ka when there is a large surge in the amount of grains matched to the LIS. This pattern suggests more IIS bergs than LIS bergs melted out over this area after 18 ka. Small IIS bergs may have been more influenced by the BG and TPD while larger LIS bergs may have been steered by deeper currents. Also, the IIS is represented by several different source areas, increasing the chance a berg from one of them melted out. The LIS is represented only by Banks Island. Source area peaks do not necessarily correspond to peaks in the amount of coarse material in the sample, but are typically within a few centimeters of each other. Differences between the graphically determined and calculated peak centers for the age v. weighted percent plots are miniscule (Table 5).

The high rate of sedimentation in deglacial periods is apparent in Figure 15. All events are less than 2 ka in duration for both ice sheets, and are therefore due to the activities of ice streams or rapid glacial collapse. The simultaneous IIS and LIS events have comparable durations, which suggests both are responding simultaneously to a long-term change.

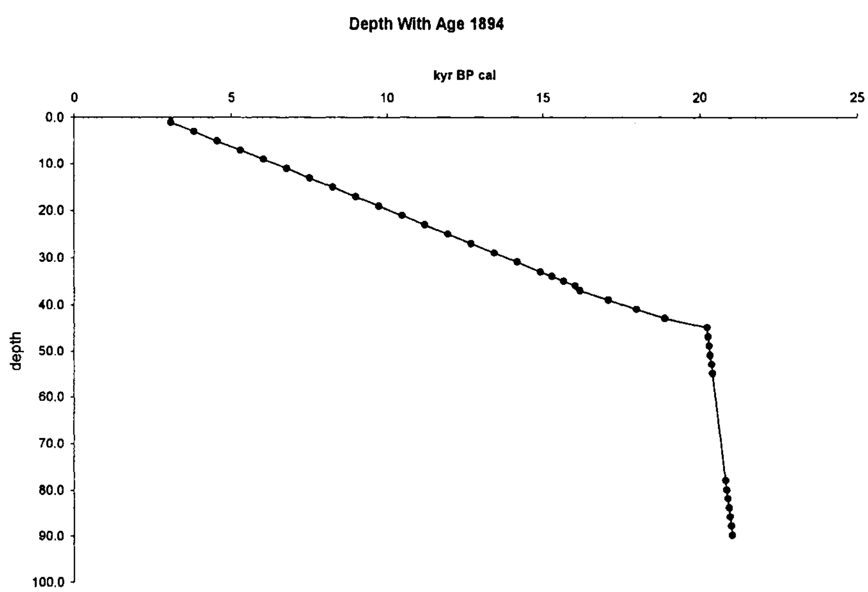

Figure 15. Depth vs. age plot for 1894. This core has a fairly linear sedimentation rate until around 19.5 kyr BP, and very rapid sedimentation below this depth perhaps corresponding to deglaciation.

Six IIS peaks and four LIS peaks can be seen in 94BC28 (Figure 16; Figure 17; Table 6). All but the simultaneous event around 45 ka have a long spacing. There is a change in sedimentation rate around 15 ka (Figure 18) thus the LIS peak around 13 ka may be an event separate from the IIS peak around 22 ka.

Comparison Of Fe Grain Peaks in Cores Across the Arctic

The presence of lone events in cores that underwent additional analysis may be due to poor preservation of companion events. In order to see if this is true, the reanalyzed cores are compared with other cores from different areas of the Arctic (Table 1). These additional cores were not considered for analysis because their geographic location wasn't ideal for capturing all IRD events, and dating was not as good compared to the cores that were further analyzed. They are presented here to see if the apparent lone events are coupled in other areas along berg drift tracks.

The graphs of other Arctic cores (Appendix B) show that the preservation of IRD events varies with geographic area. All cores with the exception of B15 and P6 show close-spaced calving events and far-spaced events possibly due to circulation changes or ice rafting. B15 shows only long-term events. All cores except P6 have been dated and are plotted as 3-point average weighted percent vs. age. P6 has not been radiocarbon dated, but the boundaries for MIS-2 have been established using lithic- and bio-stratigraphy (Polyak et al., 2003) and all peaks shown in this core are from MIS-2. Table 7 summarizes the IIS peaks in these cores, and Table 8 summarizes the LIS Peaks.

The relationship between the Laurentide and Innuitian is not clear-cut in the cores that haven't undergone additional analysis. Not all calving events are seen in each core,

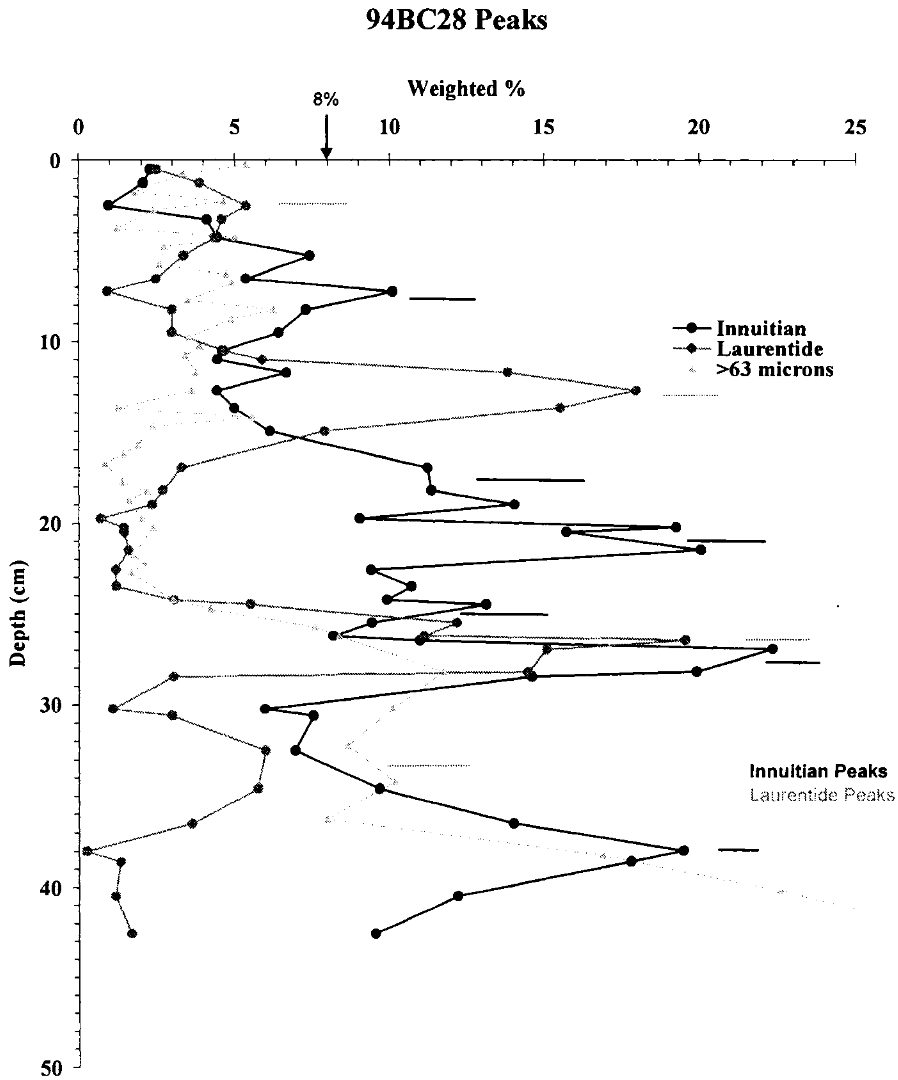

Figure 16. Comparison of weighted percent of Fe grains matched to Innuitian and Laurentide sources in core 94BC28 from Fram Strait. Coarse fraction is also shown.

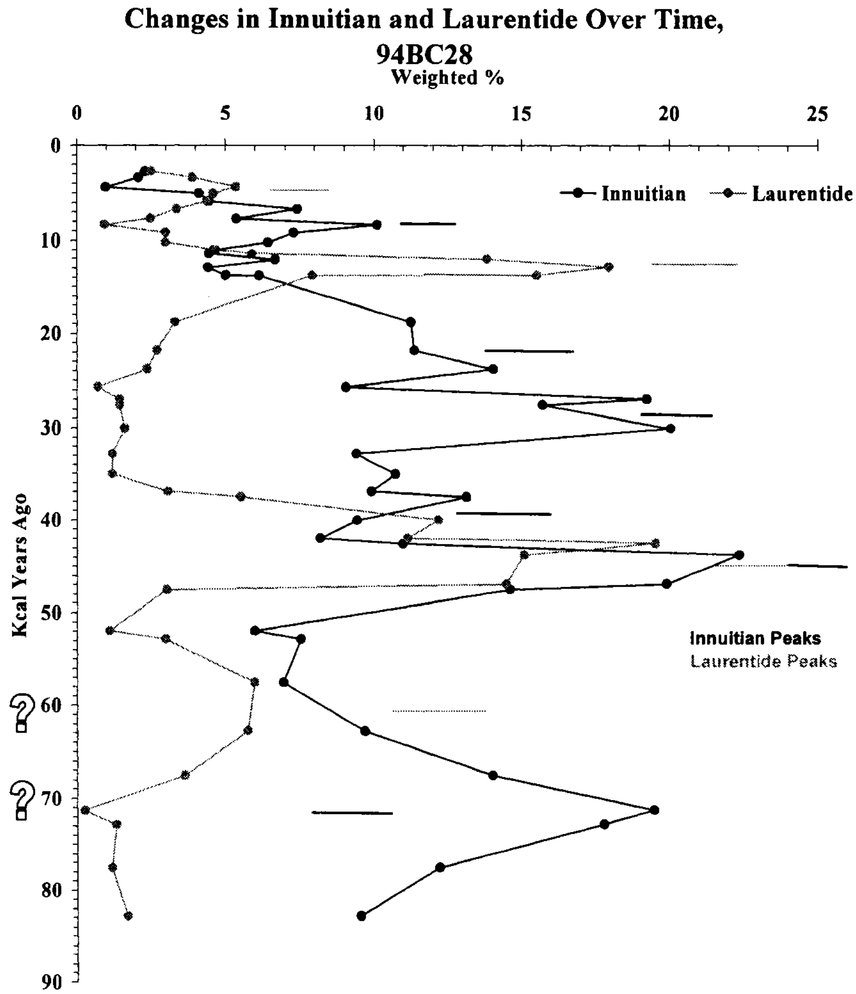

Figure 17. Changes in Fe grains from IIS and LIS plotted against radiocarbon calendar years, 94BC28. Ages below 50 Kcal are extrapolated beyond the age limit for radiocarbon dating and are highly speculative.

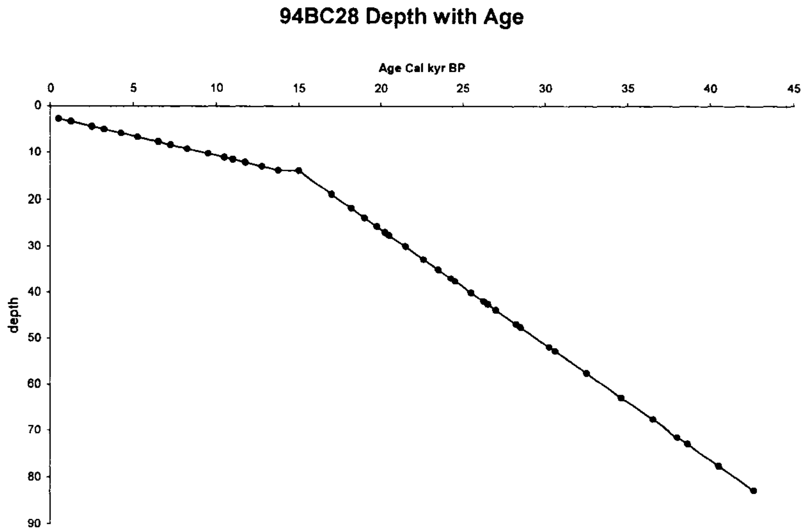

Figure 18. Age model for 94BC28.

and some calving events have multiple peaks in high-resolution cores, like Core P1/B3 below 12 ka (Figure 19).

In 94BC20 the paired Fe grain peak (LIS and IIS) that occurs between 26 and 28 ka is the only pair whose spacing suggests both ice sheets were reacting to the same trigger (Figure 20). The corresponding LIS event at this time is below significance. Thus preservation of coupled events is poor in the Wrangel Basin, with typically only one of the two ice sheet collapse events being preserved. Evidence for a 10 ka event is weak. Core 94BC08 (Figure 19; Figure 26, Appendix B) is the only core to show IRD event 6. The IIS leads paired events around 5, 7, 29, and 35.5 ka. A pair of IIS and LIS peaks below significance around 9ka is also led by an IIS peak. An event around 12 ka shows a large LIS peak but the accompanying IIS peak is below significance. The prominent LIS

Table 6. Summary of peaks in 94BC28 from the Lomonosov Ridge. Peaks at 33.25 cm and 38 cm dbsf occur below age model limits (BML) for Fairbanks. Speculative dates are shown in Figure 17.

	depth v. wt %		age v. wtd %			
IIS	3/4 peak center cm dbsf	peak width in cm	Peak center calculated from age model	Peak center determined graphically	Difference in Ka	Duration in kyr
	7.5	1.25	8.57	8.25	0.32	1.5
	17.5	2.25	20.11	22	1.89	8.5
	21.	2	28.86	28.75	0.11	4.75
	25	1.5	38.86	39.25	0.39	4
	27.75	1.5	45.74	45	0.74	5
	38	3.75	BML	BML		
depth v. wt %			age v. wtd %			
LIS	3/4 peak center cm dbsf	peak width in cm	Peak center calculated from age model	Peak center determined graphically	Difference in Ka	Duration in kyr
	2.25	1.5	4.196	4.75	0.55	1.5
	13	3.5	13.15	12.75	0.4	2
	26.5	1	42.61	45	2.39	5
	33.25	4	BML	BML		

Table 7. Summary of IIS peaks in the additional cores. Significance is a weighted percent of 8 or greater. Durations in kyr are based on interpolated ages and do not reflect the rapid changes in sedimentation rates associated with deglaciation.

Core Number	Peak center (ages or depth)	Is peak significant?	Duration (ages or depth)	Lone event?
94BC20	8.75 ka	Yes	1 ka	Yes
	13.75 ka	Yes	1.75 ka	Maybe
	27.25 ka	Yes	2.25 ka	No
94BC08	5.5 ka	Yes	0.9 ka	No
	7.1 ka	Yes	0.9 ka	No
	9.5 ka	No	0.9 ka	No
	11.3 ka	No	0.5 ka	No
	29.5 ka	Yes	8 ka	No
	35.75 ka	Yes	1.5 ka	No
B15	5.5 ka	Yes	3.25 ka	No
	11.75 ka	Yes	2.25 ka	No
	15.25 ka	Yes	2 ka	Yes
	21.25 ka	Yes	4.5 ka	Yes
	25.75 ka	Yes	2.5 ka	No
P6	10.2 cm	Yes	4 cm	No
	19 cm	Yes	6 cm	No
	30.5 cm	Yes	5 cm	No
	38 cm	Yes	3.5 cm	No
P1/B3	9.5 ka	Yes	1.2 ka	No
	11.75 ka	Yes	1 ka	Yes
	13.25 ka	Yes	0.8 ka	No
	14.6 ka	Yes	0.6 ka	No
	15.2 ka	Yes	0.8 ka	Yes

Table 8. Summary of LIS peaks in the additional cores. Significance is a weighted percent of 8 or greater.

Core Number	Peak center	Is peak significant?	Duration	Lone event?
94BC20	3.25 ka	Yes	4.25 ka	Yes
	11 ka	Yes	1.9 ka	Maybe
	26.75 ka	No	2.5 ka	No
94BC08	5 ka	Yes	1.5 ka	No
	7 ka	Yes	1 ka	No
	8.25 ka	No	1.5 ka	No
	12 ka	Yes	2 ka	No
	28.6 ka	Yes	11.25 ka	No
	35.5 ka	Yes	1.5 ka	No
B15	4.75 ka	Yes	2 ka	No
	12 ka	Yes	5 ka	No
	25 ka	Yes	2.5 ka	No
P6	15 cm	Yes	5 cm	No
	26.5 cm	Yes	3 cm	No
	31.5 cm	Yes	5 cm	No
	42 cm	Yes	8 cm	No
P1/B3	9.75 ka	Yes	0.6 ka	No
	10.7 ka	Yes	1 ka	Yes
	12.8 ka	Yes	0.5 ka	Yes
	13.8 ka	Yes	0.8 ka	No
	14.8 ka	Yes	0.6 ka	No

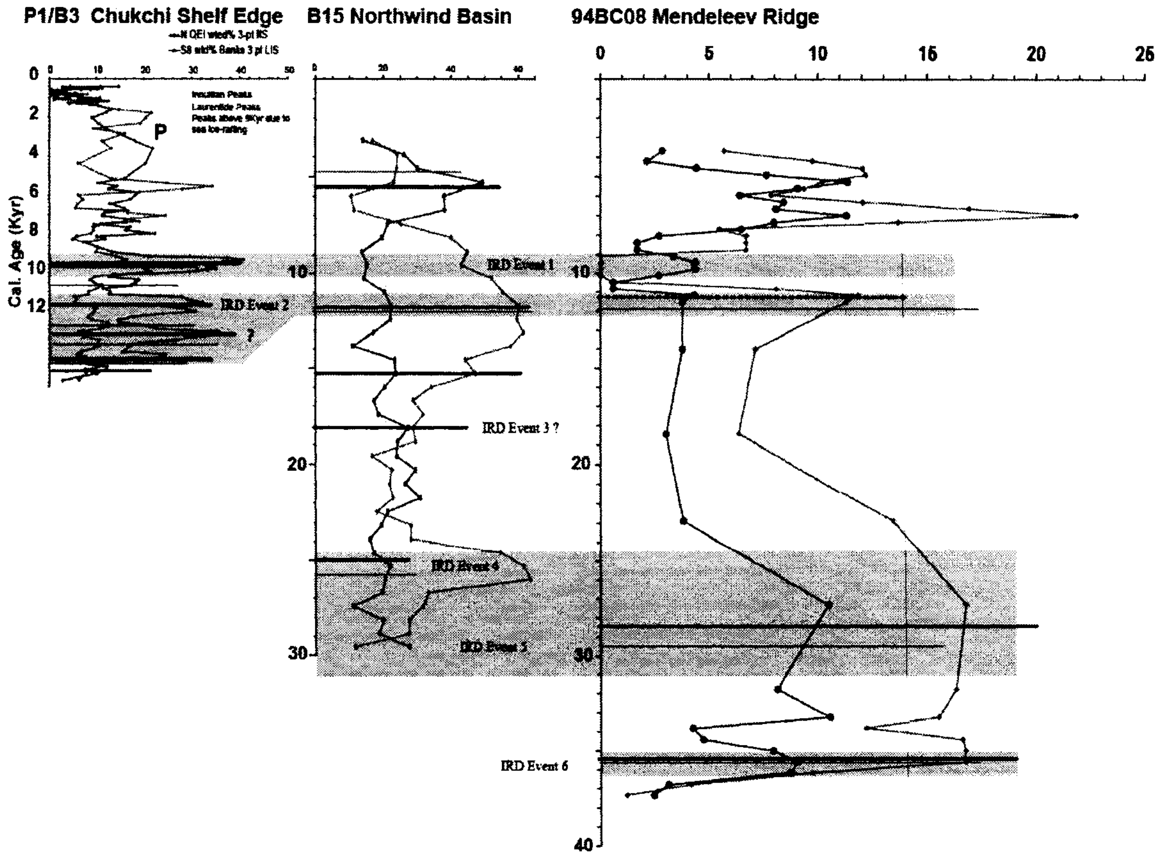

Figure 19. Correlation of calving events in additional cores.

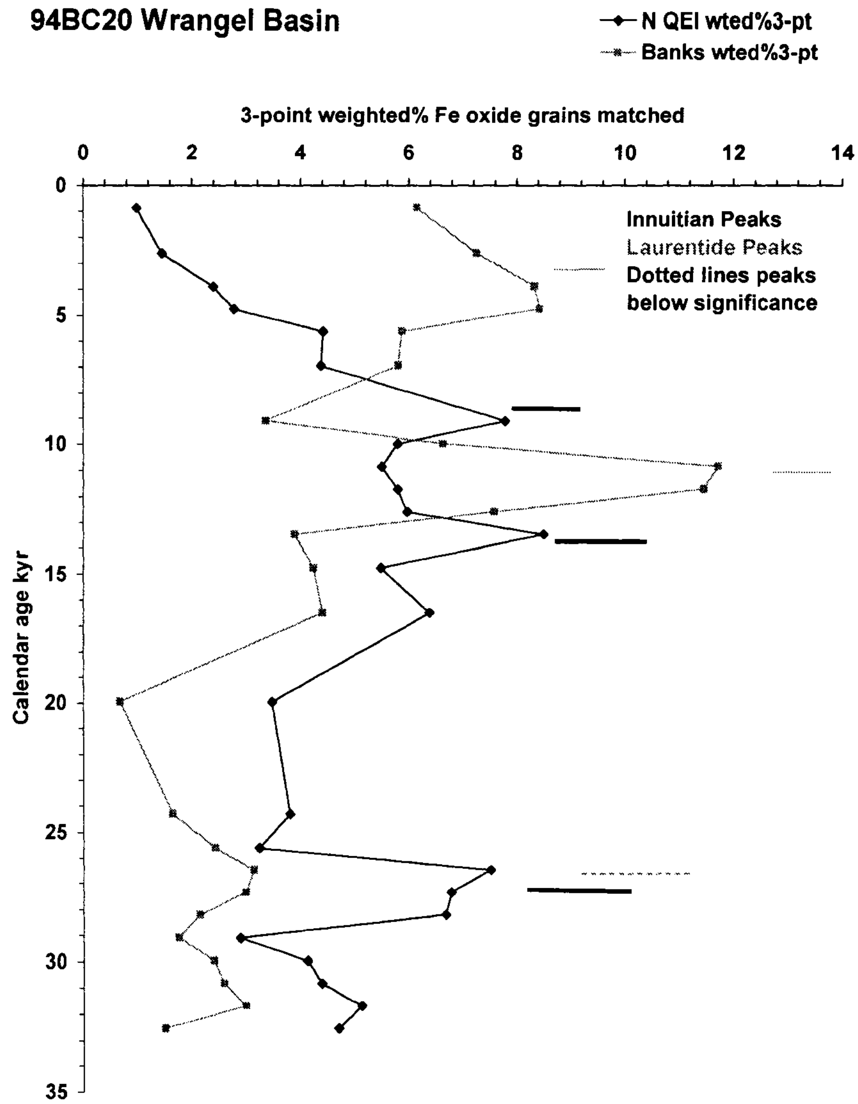

Figure 20. Changes in Fe grains from IIS and LIS plotted against radiocarbon calendar years, 94BC20.

peak around 12 ka is leading the insignificant IIS peak at this time.

Possible explanations for this reversal in peaks are that the LIS was leading the IIS (possibly by streaming through the M'Clure Ice Stream), or the IIS responded first but evidence of that early response was not preserved. This pair is not preserved at all in PS1230, only an LIS event is seen around this time in cores 94BC28, 94BC17 and 94BC20. The lack of preservation of IRD 1 at 10 ka may indicate it was smaller than previous events, which are better preserved in the Fram Strait cores. Simultaneous IIS and LIS events occur around 10.8 ka in 1894, and only an IIS event is seen in 1231 at 12 ka, though an IIS and LIS event occurs simultaneously at 13.5 ka. Comparison with other cores suggests that this was a simultaneous event whose IIS component was much smaller than the LIS, thus leading to poor preservation in some of the cores. Bergs may have been diverted around the 94BC08 core site (Figure 3), giving an apparent LIS lead. This diversion could have been caused by any number of situations ranging from grounded ice on the Chukchi borderland, changes in paleocurrents due to the Arctic Oscillation or local effects.

In B15 from the Northwind Basin, the IIS leads the LIS events around 15, 18, and 25 ka, but the peaks are not very large except for the LIS peak at 25 ka (Figure 19). The Laurentide leads the IIS event around 12 ka. The two lone IIS events seen in B15 at 15.52 and 19.75 ka would suggest that this area has problems with preserving both events in a couplet.

P6 (Figure 29, Appendix B) has much less resolution in MIS-2 than the other cores which haven't been reanalyzed, and it has not been radiocarbon dated. However, it shows four clear peaks for the IIS and three strong peaks and one insignificant peak from the LIS. The LIS is always leading in P6. P6 is close to B15, which shows similar LIS leads that are not seen in cores from different geographic areas.

In P1/B3 (Figure 21; Figure 27 Appendix B) the LIS appears to lead the IIS events between 9 and 10 ka ago and 14 and 15 ka ago. Between 12 and 14 ka ago, there is an IIS peak sandwiched between two LIS peaks. The IIS is either leading the uppermost LIS peak, or lagging the lowermost LIS peak. This core has very high resolution, and some of the confusion may have been due to how the peaks were picked (smaller peaks consisting of a single data point were assumed to be part of larger peaks consisting of multiple peaks). There is evidence for a 10 ka LIS event. This LIS event is followed by an IIS event, a pattern not seen in the Fram Strait cores. IRD Event 1 is represented by several Fe oxide grain peaks in this core (Figure 16). The sequence and number of Fe grain peaks from both the IIS and the LIS at this and other Chukchi Borderland sites is probably strongly influenced by the effect of large ice masses grounding here. These ice masses most likely originated from the LIS (Polyak et al., 2007) and would have carried Fe grains from LIS source areas. In addition to diverting floes, these grounded ice masses would have deposited LIS Fe grains in multiple peaks due to seasonal or occasional melt events at this site or to reworking of previously deposited sediment by the grounded ice.

Causes of Leads and Lags: Ramifications for Collapse Events

Six Arctic IRD events can be surmised from the cores used for this study (Table 10). Not all cores show each event. Some events are only represented by a Fe grain peak from one ice sheet, and others occur simultaneously (Table 11). Some events—such as IRD 2 in P1/B3 (Figure 21)—contain many peaks and do not give a clear signal as to

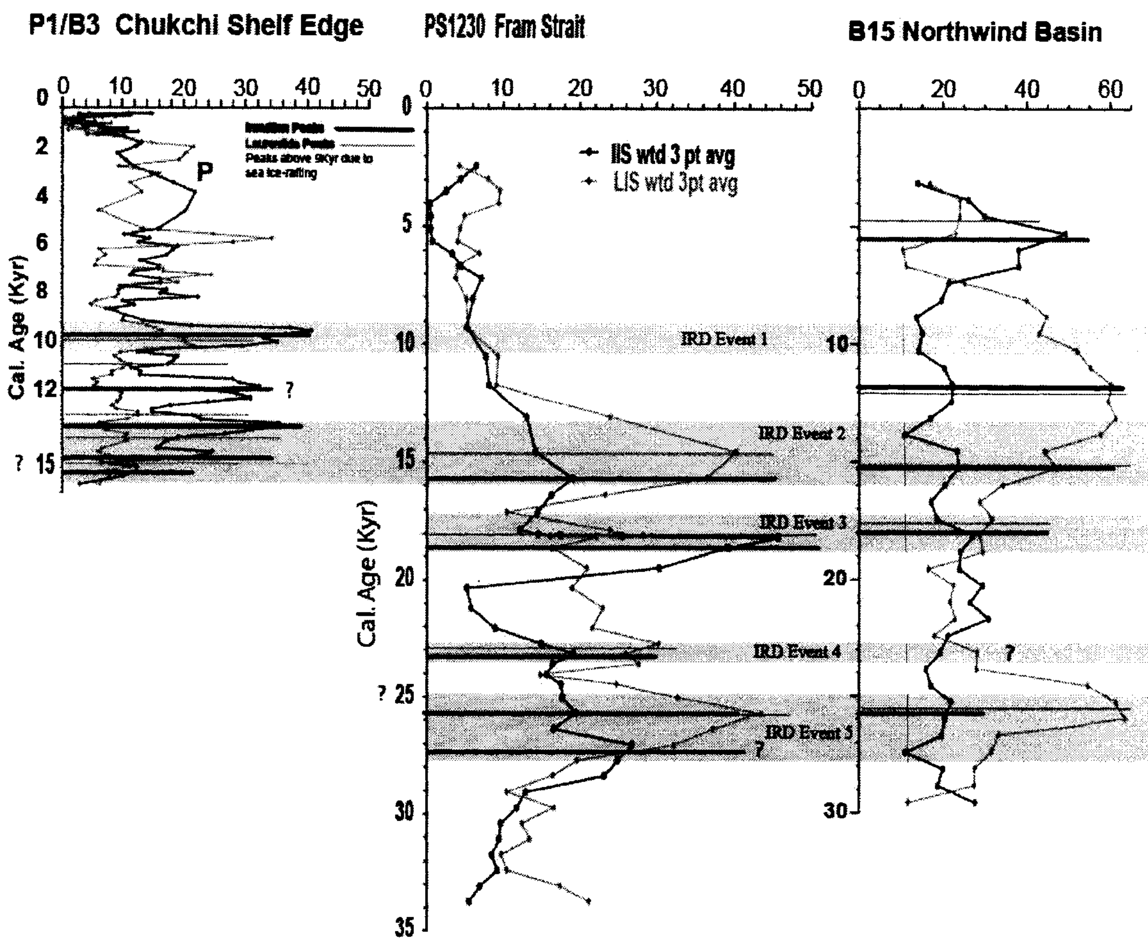

Figure 21. Correlation of IRD events across three different geographic regions. Note IRD Events 1 and 2 are best represented in the Chukchi Borderlands. The ages older than 8 ka in P1/B3 are speculative as are the correlations to peaks in this interval.

Table 9. Summary of IRD events 1 through 6. Only paired events where both IIS and LIS were significant were used to count the number of Events and IIS leads. Average duration and thickness was obtained from cores that underwent additional analysis with the exception of Event 6, which is only present in 94BC08.

IRD Event	Average Event Age	Number of cores used to obtain age	Number of cores containing this event (out of 9)	Number of cores showing IIS Lead	Average duration in kyr, (thickness in cm) IIS	Average duration in kyr, (thickness in cm) LIS
1	11.5 ka	3	3	1	3, (2)	1.75, (2.5)
2	15 ka	3	6	3	1.75, (2.1)	1.13, (2.25)
3	18 ka	3	3	3	2, (4.13)	1.5, (3.45)
4	23-24 ka	2	2	1	2.63, (2)	1.13, (3.13)
5	26-29 ka	3	4	4	2, (3)	1.9, (3)
6	~36 ka	1	1	1	1.5	1.5

Table 10. Spacing between Laurentide and Innuitian events in individual cores. Only significant peaks with spacing of 1 cm or less are listed. Simultaneous spacing refers to events whose spacing is so close they appear to occur simultaneously on the depth v. weighted percent graphs.

Core	Spacing between events (cm)	Average LIS event age (kyr)	Average depth of LIS event (cm)
PS1230	.25	22.5	30.5
PS1231	Simultaneous	14	13.5
PS1231	1	16	18.5
PS1231	1	23.5	29.5
1894	Simultaneous	11	21
P6	.25	Core not dated	40.5
B15	.5	4.75	3
B15	.5	12	12
B15	.75	25	32
94BC08	Simultaneous	5	9.5
94BC08	Simultaneous	7	26
94BC08	Simultaneous	38.5	31.5

which ice sheet is leading and which is lagging. The timing of peaks was not the same across cores, which could be due to difficulties in correlating dates across different parts of the Arctic. On average, IIS events had broader peaks than LIS events perhaps because more source areas contribute to the IIS signal, leading to better preservation of IIS events.

The best-dated pair is centered around 18 ka in core PS1230. These two events were separated by 0.25 cm in the weighted percent v. depth plot, which is a separation of roughly 250 years. (The core was sampled at a 1 cm interval, the distance between event peaks was determined graphically.) This event correlates to IRD event 3. The simultaneous events in PS1231 and 1894 are IRD Event 1. The simultaneous event around 31.5 cm in 94BC08 is IRD event 6. The closely spaced events in B15 around 12 and 32 cm may be IRD Event 1, and either IRD Event 4 or IRD Event 5 respectively depending on the age model accuracy.

There is still uncertainty as to whether glacial collapse is caused by internal glacial mechanisms or changes in climate and/or ocean circulation. There is some evidence that smaller ice sheets are either able to trigger the collapse of larger ice sheets, or respond first to the external forcing mechanism that triggers collapse (Fronval et al., 1995; Scourse et al., 2000; and Grousset et al., 2000; Marshall and Kourtnik, 2006). Smaller ice sheets may be more sensitive to climatic forcing, causing their margins to become more unstable than those of larger ice sheets with slower response times. If the small ice sheet is already in an unstable state, slight changes in thermal regime or the position of the grounding line can cause rapid collapse. The collapse of the small ice sheet may cause destabilization of the margins of the larger ice sheet, thus triggering rapid streaming in larger ice sheets. These larger ice sheets are slower to respond than smaller ones, and they are perhaps destabilized by the freshwater inputs of melting bergs from the smaller ice sheets. Peck et al. (2007a) suggested that a freshening of the North Atlantic surface waters, and the resulting reduction in the strength of the Atlantic Meridional Overturning Circulation (AMOC) (caused by melting European ice sheets) would lead to increased ice shelf growth at the margins of the LIS. These shelves would then ablate due to reductions in meridional overturning, triggering ice sheet collapse. Flückinger et al. (2006) speculated that a collapse of the meridional overturning current would cause sea level rises (due to sea water expansion) and subsurface warming in the North Atlantic (through downward diffusion of heat). The initial sea level rise would destabilize the sensitive margins of marine ice sheets, causing collapse and a greater input of fresh water, increasing the subsurface warming. This feedback loop would act to trigger a surge from the larger LIS. The system would reset when the feedback loop breaks down and a new equilibrium is reached.

Work on European precursors to Heinrich events using ODP cores 644, 609 and V23-81 (Fronval et al. 1995) shows that decreases in temperature over Greenland correlates to increases in European IRD events, suggesting that small ice sheets are early responders to climactic changes that bring about deglaciation. The sensitivity of ice shelves to ocean warming was tested by Walker et al. (2007) using a simplified model of an idealized Filchner Ice Shelf (Antarctica). The model was run until the ice shelf reached an equilibrium state. Warmer oceans produced more rapid changes in equilibrium mass balance. Experiments with velocity also found that while the control experiment reached equilibrium in 490 years, a fast-flowing ice shelf could reach equilibrium within 200 years. Recent observations of the Greenland and Antarctic ice sheets indicate that ice sheets can respond very quickly to external forcing due to regional changes in oceanic or atmospheric warming. These rapid changes were not predicted by models, and there is still uncertainty surrounding their cause (Bamber et al., 2007).

One would expect many large-scale LIS events to have smaller ice sheet precursors, like those seen in the IIS for Arctic events and the British Ice Sheet and Fennoscandinavian Ice Sheet for Heinrich events. The data from the Arctic would seem to bolster the claim that Heinrich precursor events can be seen in smaller ice sheets. In the cores used in this study, the smaller IIS appears to almost always lead paired events. The IIS lead suggests that the ice calved during IIS events may have been sufficient to destabilize the marine component of the Arctic IIS. Unfortunately current models are unable to accurately predict how the grounding line of a marine ice sheet would respond to changes in sea level (Vieli and Payne, 2005).

The prevalence of IIS leads in cores PS1230, PS1231, 1894, 94BC08, and B15 shows that small ice sheets either respond first to climatic forcing or that changes (such as binge/purge cycles, loss of a buttressing ice shelf, streaming, and changes in basal conditions) in small ice sheets can be transmitted to larger ice sheets by changes in sea level, perturbation of ocean circulation, or through the direct interaction of a large ice sheet and a smaller buttressing ice sheet. The lag times of closely spaced events (between 0.25 and 1 ka apart) suggests the response was fairly rapid. In order to respond so quickly, the larger LIS had to be at a tipping point where a slight change could result in increased calving.

The timing of closely spaced events would also suggest that the LIS sometimes lagged the IIS at times much shorter than the span of a Bond cycle. Combinations of climate and ice sheet dynamics have also been proposed as a cause of H events by Peck et al. (2006), with the internal dynamics of an unstable British Ice Sheet causing collapses that release large meltwater pulses which weaken AMOC. A coupled climate model (Wang and Mysak, 2006) confirms the importance of sea ice and salinity in AMOC mode changes. Arctic ice sheets were not specifically addressed by these authors, but may have similar impacts on ocean mixing. Peck et al. (2007a) also proposed that instabilities in the Northern European Ice Sheets may have triggered the reductions of the North Atlantic thermohaline circulation seen prior to H1and H2.

The idea of small ice sheet precursors is still controversial. Precursor evidence was contested by Peck et al. (2007b) whose work on MD01-2461 found a 2-kyr periodicity to European Ice Sheet IRD. This periodicity suggested that millennial scale fluctuations in smaller ice sheets was common, and that since the Northwestern European Ice Sheets were at a juvenile stage during H4 and H5, small ice sheet instabilities could not have been the trigger for Laurentide destabilization. At the time of this printing, this controversy has not been resolved.

While a case can be made for the IIS being an early responder to climatic forcing, it must be remembered that the IIS and LIS coalesced during the LGM. This coalescence would make it easier for changes in the internal dynamics of the IIS to be transmitted to the LIS. Buttressing ice shelves appear to play an important role in glacial stability (De Angelis and Skvarca, 2003; Dupont and Alley, 2005; Hulbe et al., 2005; Stokes, personal communication 2006). As the IIS collapsed, the LIS would behave as if it had lost an ice shelf. The loss of the buttress would cause the LIS to surge in areas that allowed for streaming, resulting in an LIS signal appearing at the same time or shortly behind an IIS signal. This appears to be the case for the events listed in Table 10, in particular those that occurred simultaneously. However, the loss of a buttress along an outlet channel such as M'Clure Strait or Viscount Melville Sound has never been modeled and has no modern analog. Thus, the possibility that LIS calving events were caused by the loss of a buttressing IIS is somewhat speculative.

LIS leads appear to be an anomaly. Two of the three LIS leads seen in pairs with a spacing of 2 ka or less occurred in P1/B3 and B15, both cores from near the Northwind Ridge. The other LIS lead is seen in PS1231 at 15 ka, and may be due to sampling error as no other Fram Strait core shows an LIS lead at this time. Of the four LIS lone events, half are from P1/B3, and half are from 94BC20 (Wrangel Basin, near the Central Arctic), suggesting that the lack of IIS events may be due to geography. It would seem that the LIS was susceptible to collapse after each IIS calving event, or that both the IIS and LIS were susceptible to collapse at the same time.

CHAPTER IV

SUMMARY AND CONCLUSIONS

Peaks in Fe grain abundances from cores in the Arctic can be used to determine periods of increased calving from the LIS and IIS. Reanalysis of cores PS1230, PS1231, and 1894 from Fram Strait and 94BC28 from Lomonosov Ridge show that there have been six Arctic collapse events at 10, 15, 18, 22.9, 26, and 48 ka. Of the collapse events with both a preserved IIS and LIS component in each core, the IIS lead occurs in four of four in PS1230, two of four in PS1231, two of three in 1894, and one of two in 94BC17. The LIS and IIS Fe grain peaks occurred simultaneously once in PS1231, once in 1894, and once in 94BC17. The evidence for an IIS lead is bolstered by data from additional cores showing that in the majority of calving events, the IIS either leads the LIS or the timing of the events is so close they are considered simultaneous.

It was recently suggested that the IIS grew late in the Wisconsinan after the lowering of the eustatic sea level had reached a maximum and the LIS had split the mid-latitude jet stream, bringing necessary moisture to the IIS area (England et al., 2006). This argument is bolstered by a lack of deglacial landforms in the northwestern QEI older than 11 ka BP. However, the large peaks in ferromagnetic IRD grains that can be traced to the IIS area prior to 10 cal ka suggest that the IIS has existed prior to this last glaciation in OIS 2. In fact, large peaks of Fe grains from this ice sheet are seen as far back as 48 ka and there are five collapses of the IIS since 48 ka time.

The volume of ice needed to produce these peaks could not have come solely from sea ice. IIS peaks tend to have comparable percentages to LIS peaks. The flux of icebergs passing through Fram Strait needed to produce the IRD events seen in PS1230 is estimated to be 300-1000 km^3a^{-1} (Darby et al., 2002). The contribution of the M'Clure Strait Ice Stream is estimated at a minimum of 400 km^3a^{-1} (Stokes et al., 2005). All core sites are far north of the modern maximum southern limit of icebergs (Andrews, 2000) and are north of the LGM limit for quasi-permanent sea ice (de Vernal et al., 2005) in particular 94BC28, which is near the center of the Arctic Ocean. In addition, even the Fram Strait core sites were well north of the limits of perennial ice during glacial intervals. Thus near complete melting of only a few bergs or all sea ice can be eliminated as a cause for these Fe grain peaks from either the IIS or LIS

The findings of this study are summarized as follows:

1. Nineteen events with a significant IIS and LIS component were identified. Of these fourteen within 2 ka of each other were identified and twelve events had a spacing of 1 cm or less between IIS and LIS components. In IRD events 1-6, the IIS lead 68% of the time, with 26% of events in all cores occurring simultaneously. In cores showing events with a spacing of less than 1 cm, 33% of the events showed an IIS lead, and 41.7% showed the events occurring simultaneously (Table 10). IIS components of Arctic IRD events had durations of 1.5-3 kyr, while the LIS components had durations of 1.1-2 kyr. Differences in lead-time in the Fram cores may be due to inconsistencies in dating models (Especially in PS1231, where dates from PS1230 were used to construct the age model), slight changes in drift tracks, sedimentation, or reworking on the sea floor. Differences in lead-time across different geographical regions are expected.

The best age control on an IIS lead is from IRD Event 3 in PS1230. The lead-time for IRD Event 3 in PS1230 is around 250 years. PS1230, PS1231, 1894, P6, B15, and 94BC08 all have IIS and LIS events within one centimeter or less of each other on the depth v. weighted percent plots. These changes in depth represent changes in time ranging from approximately 250 to 1000 years.

2. Arctic IRD Events 1, 2, and 4 as preserved by Fe grain peaks correlate to Heinrich Events 0, 1, and 2 respectively. H-0 occurred after IRD-1, H-1 occurred before IRD-2, and H-2 occurs at the end the range for IRD-4. H-3 occurs around 1-2 ka before the earliest possible date for IRD 5, and H-4 occurs around 2 ka before IRD 6 (Peck et al., In Press). Discrepancies in correlating dates for H and Artic IRD events may be the result of the inaccuracies inherent in dating Arctic sediments.

3. Events with a short duration (up to 2.5 ka, such as all events seen in PS1230) may have been caused by ice streams; events with a long duration (over 2.5 ka, such as events occurring after 20 ka in 94BC28) may have been caused by other factors such as ocean circulation or shifting climate patterns. These long separations may also be due to changes in sedimentation rates. It is difficult to determine which is the case without better dating or cores with higher sedimentation rates.

4. Some cores that have not undergone additional analysis (94BC08, B15, P6, P1/B3) show the LIS leading an IIS event around 10 ka, which has been found to

be a time of increased Laurentide ice stream activity (Stokes et al., 2005). The LIS may have responded first to the cause of this event. This rapid purge may have acted to destabilize the IIS margins. PS1230 does not show this event. PS1231 shows an IIS event around 11.25 ka with no corresponding LIS event until 8 ka, and 1894 shows IIS and LIS events occurring simultaneously at 10.8 ka. This discrepancy between the Fram and Chukchi Borderland cores in the western Arctic may be due to local conditions. Cores showing LIS leads tend to be near the Northwind Ridge, where grounded ice may have delayed the melting of bergs, producing an atypical stratigraphy.

5. Cores from Fram Strait show the peaks with the largest number of Fe grains corresponding to IRD Events 1-5. Cores from Fram Strait are more useful for determining long-term patterns in the behavior of the IIS and LIS, even though they are far from the calving front. Since not all peaks corresponding to events are present, even in cores from the same region, it is important to compare cores from different areas when trying to determine the relationship between the IIS and LIS.

6. While the chronologic control in the Arctic cores lacks the high resolution for detailed dating of IRD events the depth vs. weight percent plots can be used for determining leads and lags. For example, if an LIS event occurs at 15.5 cm and an IIS event occurs at 16.75 cm, we can say that the IIS event is older than the LIS event. If the sedimentation rates for the area in which the core was taken and the depth at which events occur are known, a rough estimate of lead-time can be

determined using the spacing between the two events.

7. Of the nine lone events observed, only two (both IIS) occurred at the same time. These were in cores B15 and P1/B3, both of which were located near the Northwind Ridge. Lone events may be caused by random melting over the core site. This makes it necessary to compare the position of Fe grain peaks in any given core with the position of Fe grain peaks in other cores across the Arctic.

REFERENCES

Alley, R.B. (1995), Resolved: the Arctic controls global climate change, *Coast. Estuar. Studies*, *49*, 263–283.

Andrews, J.T. (2000), Icebergs and iceberg rafted detritus (IRD) in the North Atlantic: facts and assumptions, *Oceanography*, *13*(3), 100–108.

Andrews, J.T., B. Maclean, M. Kerwin, W. Manley, A.E. Jennings, and F. Hall (1995), Final stages in the collapse of the Laurentide Ice Sheet, Hudson Strait, Canada, NWT: ^{14}C AMS dates, seismic stratigraphy, and magnetic susceptibility logs, *Quat. Sci. Rev.*, *14*, 983–1004.

Backman, J., M. Jakobsson, R. Lovlie, L. Polyak, and L.A. Febo (2003), Is the central Arctic Ocean a sediment starved basin?, *Quat. Sci. Rev.*, *23*, 1435–1454.

Bamber, J.L., R.B. Alley, and I. Joughin (2007), Rapid response of modern day ice sheets to external forcing. *Earth Planet. Sci. Lett.*, *257*, 1–13.

Bauch, H.A., T. Mueller-Lupp, R.F. Spielhagen, E. Taldenkova, H. Kassens, P.M. Grootes, J. Thiede, J. Heinemeir, and V.V. Petryashov (2001), Chronology of the Holocene transgression at the northern Siberian margin, *Global Planet. Change*, *31*, 125–139.

Beck, J.W., D.A. Richards, R. Lawrence, R. Edwards, B.W. Silverman, P.L. Smart, D.L. Donahue, S. Hererra-Osterheld, G.S. Burr, L. Caloyas, A.J. Timothy, and D.B. Jull (2001), Extremely large variations of atmospheric ^{14}C concentration during the last glacial period, *Science*, *292*, 2453—2458.

Blake, W. Jr. (1970), Studies of glacial history in Arctic Canada. I. Pumice, radiocarbon dates, and differential postglacial uplift in the eastern Queen Elizabeth Islands, *Can. J. Earth Sci.*, *7*, 634—664.

Blake, W. Jr. (1992), Holocene emergence at Cape Herschel, east-central Ellesmere Island, Arctic Canada: implications for ice sheet configuration, *Can. J. Earth Sci., 29*, 1958—1980.

Blake, W. Jr. (1997), Glacial sculpture along the east-central coast of Ellesmere Island, Arctic Archipelago. *Report of Activities, Part C,* Geological Survey of Canada Paper 77-1C.

Blake, W. Jr., M.M. Boucherle, B. Fredskild, J.A. Janssens, and J.P. Smol (1992), The geomorphological setting, glacial history and Holocene development of 'Kap Inglefield So', Inglefield Land, North-West Greenland, *Meddelelser om Gronland, Geosci.*, *27,* 1—42.

Bond, G.C., and R. Lotti (1995), Iceberg discharges into the North Atlantic on Millennial time scales during the Last Glaciation, *Science*, *267*, 1005—1010.

Bond, G.C., W. Showers, M. Elliot, M. Evans, R. Lotti, I. Hajdas, G. Bonani, and S. Johnson (1999), The North Atlantic's 1-2 kyr climate rhythm: relation to Heinrich events, Dansgaard/Oeschger cycles and the Little Ice Age, *Mechanisms of Global climate change at millennial timescales, Geophysical Monograph, 112*, 35—58.

Brigham-Grette, J., L.M. Gualteri, O. Glushkova, Yu., T.D. Hamilton, D. Mostoller, and A. Kotov (2003), Chlorine-36, and ^{14}C chronology support a limited last glacial maximum across central Chukota, northeast Siberia, and no Berengian ice sheet, *Quat. Res.*, *59*, 386—398.

Broecker, W.S. (1994), Massive iceberg discharges as triggers for global climate change, *Nature, 372*, 421—424.

Clark, C.D, and C.R. Stokes (2001), Extent and basal characteristics of M'Clintock Channel Ice Stream. *Quat. Int.*, *86*, 81—101.

Clark, D.L., R.R. Whitman, K.A. Morgan, and S.D. Mackey (1980), Stratigraphy and glacial-marine sediments of the Amerasian Basin, Central Arctic Ocean, *Geol. Soc. Am., Special Paper 181*.

Dansgaard, W., S.J. Johnsen, H.B. Clausen, D. Dahl-Jensen, N.S., Gundestrup, C.U. Hammer, C.S. Hvldberg, J.P. Steffensen, A.E. Sveinbjornsdottir, J. Jouzel, and G. Bond (1993), *Nature*, *364*, 218—220.

Darby, D.A. (2003), Sources of sediment found in sea ice from the western Arctic Ocean, new insights into processes of entrainment and drift patterns. *J. Geophys. Res.*, *108*(C8). 13-1—13-10.

Darby, D.A., A.S. Naidu, T.C. Mowatt, and G.A. Jones (1989), Sediment composition and sedimentary processes in the Arctic Ocean, in *The Arctic Seas: Climatology, Oceanography, Geology, and Biology* edited by Y. Herman, VanNostrand Reinhold, New York, 657—720.

Darby, D.A. and J.F. Bischof (1996), A statistical approach to source determination of lithic and Fe-oxide grains: an example from the Alpha Ridge, Arctic Ocean. *J. Sed. Res., Sec. A, Sed. Pet. Proces.*, *66*, 599—607.

Darby, D.A., J.F. Bischof, and G.A. Jones (1997), Radiocarbon chronology of depositional regimes in the western Arctic Ocean. *Deep-Sea Res. II*, *44*(8), 1745—1757.

Darby, D.A., J.F. Bischof, R.F. Spielhagen, S.A. Marshall, and S.W. Herman (2002), Arctic ice export events and their potential impact on global climate during the late Pleistocene. *Paleoceanography*, *17*(2),15—17.

Darby, D.A. and J.F. Bischof (2004), A Holocene record of changing Arctic Ocean ice drift analogous to the effects of the Arctic Oscillation. *Paleoceanography*, *19*, PA 1027, doi:10.1025/2003PA000961.

Darby, D.A., L. Polyak, and H. Bauch (2006), Past glacial and interglacial conditions in the Arctic Ocean and marginal seas--a review, *Prog. Oceanograp.*, *71*, 129—144.

De Angeles, H., and P. Skvarca (2003), Glacier surge after ice shelf collapse, *Science*, *299*, 1560–1562.

De Vernal, A., F. Eynaud, M. Henry, C. Hillaire-Marcel, L. Londeix, S. Mangin, J. Mathiessen, F. Marret, T. Radi, A. Rochon, S. Solignac, and J.-L. Turon, (2005), Reconstruction of sea-surface conditions at the middle to high latitudes of the Northern Hemisphere during the Last Glacial Maximum (LGM) based on dinoflagellate cyst assemblages, *Quat. Sci. Rev.*, *24*, 897—924.

Dupont, T.K., and R.B. Alley, (2005), Assessment of the importance of ice-shelf buttressing to ice-sheet flow, *Geophys. Res. Lett.*, *32*, LO4503, doi:10.1092/2004GL022024.

Dyke, A.S., J.T. Andrews, P.U. Clark, J.H. England, G.H. Miller, J. Shaw, and J.J. Veillette, (2002), The Laurentide and Innuitian ice sheets during the Last Glacial Maximum, *Quat. Sci. Rev.*, *21*(1-3), 9—31.

Dyke, A.S., R. McNeely, J.T. Andrews, W.R. Peliter, J.J. Clague, J.H. England, and J.-M. Gagnon, (2003), Preliminary assessment of Canadian marine reservoir ages. CANQUA-CGRG Abstract.

England, J. (1998), Support for the Innuitian Ice Sheet in the Canadian High Arctic during the Last Glacial Maximum, *J. Quat. Sci.*, *13*(3), 273—280.

England, J. (1999), Coalsecent Greenland and Innuitian ice during the Last Glacial Maximum: revising the Quaternary of the Canadian High Arctic, *Quat. Sci. Rev.*, *18*, 421—456.

England, J. N. Atkinson, J. Bednarski, A.S. Dyke, D.A. Hodgson, and C.O. Cofaigh, (2006), The Innuitian Ice Sheet: configuration, dynamics and chronology, *Quat. Sci. Rev.*, *25*, 689—703.

Fairbanks, R.G., R.A. Mortlock, T.-C. Chiu, L. Cao, A. Kaplan, T.P. Guilderson, T.W. Fairbanks, A.L. Bloom, P.M. Grootes, and M.-J. Nadeau (2005), Radiocarbon calibration curve spanning 0 to 50,000 years BP based on paired $^{230}Th/^{234}U/^{238}U$ and ^{14}C dates on pristine corals, *Quat. Sci. Rev.*, *24*, 1781—1796.

Flückinger, J., R. Knutti, and J.C.W. White (2006), Oceanic processes as potential trigger and amplifying mechanisms for Heinrich events, *Paleoceanography*, PA2014, doi:10.1029/2005PA001204.

Fronval, T, E. Jansen, J. Bloemendal, and S. Johnsen (1995), Oceanic evidence for coherent fluctuations in Fennoscandian and Laurentide ice sheets on millennium timescales, *Nature*, *374*, 443—446.

Grousset, F.E., E. Corijo, S. Huon, L. Herve, T. Richter, D. Burdloff, J. Duprat, and O. Weber (2001), Zooming in on Heinrich layers, *Paleoceanography*, *16*(3), 240—259.

Grousset, F.E., C. Pujol, L. Labeyrie, G. Auffret, and A. Boelaert (2000), Were the North Atlantic Heinrich events triggered by the behavior of the European Ice sheets?, *Geology*, *28*(2), 123—126.

Hulbe, C.L., D.R. MacAyeal, G.H. Denton, J. Kleman, and T.V. Lowell (2005), Catastrophic ice shelf breakup as the source of Heinrich event icebergs, *Paleoceanography*, *19*, 1004—1029.

Jakobsson, M., J. Backman, A. Murray, and R. Lovlie (2003), Optically stimulated luminescence dating supports central Arctic Ocean cm-scale sedimentation rates, *Geochem., Geophys., Geosyst.*, *4*(2),1016—1027.

Jakobsson, M., R. Lovlie, H. Al-Hanbali, E. Arnold, J. Backman, and M. Morth (2000), Manganese and color cycles in the Arctic Ocean sediments constrain Pleistocene chronology, *Geology*, *28*(1), 23—26.

Johnson, R.G., and S.E. Lauritzen (1995), Hudson Bay—Hudson Strait jokulhaups and Heinrich events: a hypothesis, *Paleogeo., Palaeoclim., Palaeoeco.*, *117*, 123—137.

MacAyeal, D.R. (1993), Binge/purge oscillations of the Laurentide Ice Sheet as a cause of the North Atlantic's Heinrich events, *Paleoceanography*, *8*(6), 775—784.

Mangerud, J., V. Astakhov, and J.-I. Svendsen (2002), The extent of the Barents-Kara ice sheet during the Last Glacial Maximum, *Quat. Sci. Rev.*, *21*, 111—119.

Marshall, S.J., and G.K.C. Clark (1997), A continuum mixture model of ice stream thermomechanics in the Laurentide Ice Sheet 2. Application to the Hudson Strait Ice Stream, *J. Geophys. Res.*, *102*(B9), 20615—20637.

Marshall, S.J., and M.R. Koutnik (2006), Ice sheet action versus reaction: Distinguishing between Heinrich events and Dansgaard-Oeschger cycles in the North Atlantic, *Paleoceanography, 21*, PA2021, doi: 10.1029/2005PA001247.

Peck, V.L., I.R. Hall, R. Zahn, H. Elderfeild, F. Grousset, S.R. Hemming, and J.D. Scourse (2006), High resolution evidence for linkages between NW European ice sheet instability and Atlantic Meridional Overturning Circulation, *Earth Planet. Sci. Lett., 243*, 476—488.

Peck, V.L., I.R. Hall, R. Zhan, and J.D. Scourse (2007a), Progressive reduction in NE Atlantic intermediate water ventilation prior to Heinrich events: Response to NW European ice sheet instabilities?, *Geochem., Geophys., Geosyst., 8*, 1, 1—11.

Peck, V.L., I.R. Hall, R. Zahn, F. Grousset, S.R. Hemming, and J.D. Scourse (2007b), The relationship of Heinich events and their European precursors over the past 60 ka BP: a multi-proxy ice-rafted debris provenance study in the North East Atlantic, *Quat. Sci. Rev., 26*,(7-8), 862—875.

Peltier, W.R. (1994), Ice age paleotopography, *Science, 265*, 195—201.

Polyak, L., D.A. Darby, J. Bischof, and M. Jakobbson (2007), Stratigraphic constraints on late Pleistocene glacial erosion and deglaciation of the Chukchi margin, Arctic Ocean, *Quat. Res., 67*, 234—245.

Polyak, L., W.B. Curry, D.A. Darby, J.F. Bischof, and T.M. Cronin (2003), Contrasting glacial/interglacial regimes in the western Arctic Ocean as exemplified by a sedimentary record from the Mendeleev Ridge, *Palaeogeo., Palaeoclim., Palaeoeco., 203*(1-2), 73—93.

Polyak, L., M.H. Edwards, M. Jakobsson, and B.J. Coakley (2001), Existence of Arctic ice shelves during the Pleistocene inferred from deep-sea glaciogenic bedforms, *Nature, 410*, 453—457.

Rashid, H., R. Hesse, and D.J.W. Piper (2003), Origin of unusually thick Heinrich layers in ice-proximal regions of the northwest Labrador Sea. *Earth Planet. Sci. Lett., 208*, 319—336.

Robinson, L. F., J.F. Adkins, L.D. Keigwin, J. Southon, D.P. Fernandez, S.-L. Wang, and D.S. Scheirer (2005), Radiocarbon variability in the Western North Atlantic during the last deglaciation, *Science, 310*, 1469—1473.

Scourse, J.D., I.R. Hall, I.N. McCave, J.R. Young, and C. Sugdon (2000), The origin of Heinrich Layers: evidence from H2 for European precursor events. *Earth Planet. Sci. Lett., 182*, 187—195.

Stokes, C., and C.D. Clark (2001), Palaeo-ice streams. *Quat. Sci. Rev., 20*, 1437—1457.

Stokes, C.R., C.D. Clark, D.A. Darby, and D.A Hodgson, (2005), Late Pleistocene ice export events into the Arctic Ocean from the M'Clure Strait Ice Stream, Canadian Arctic Archipelago, *Global Planet. Change*, *49*,139—162.

Stuiver, M., P.J. Reimer, E. Bard, J.W. Beck, G.S. Burr, K.A. Hughen, G. McCormac, J. Van Der Plicht, and M. Spurk (1998), INTCAL98 Radiocarbon age calibration, 24,000-0 cal BP, *Radiocarbon, 40*(3), 1041—1083.

Svendsen, J.I., H. Alexanderson, V.I. Astakhov, I. Demidov, J.A. Dowdeswell, S. Funder, V. Gataullin, M. Henriksena, C. Hjort, M. Houmark-Neilsen, H.W. Huggerten, I. Olfsson, M. Jakobsson, K.H. Kjaeri, E. Larsen, H. Lokrantz, J. Pekka Lunkka, A. Lyså, J. Mangeruda, A. Matiouchkov, A. Murray, P. Mölleri, F. Niessen, O. Nikolskaya, L. Polyak, M. Saarnisto, M. Siegert, R.F. Spielhagen, and R. Stein (2004a), Late Quaternary ice sheet history of northen Eurasia, *Quat. Sci.Rev.*, *23*, 1229—1271.

Svendsen, J.I., V. Gatalluin, J. Mangerud, and L. Polyak (2004b), The glacial history of the Barents and Kara Sea region, in *Quaternary Glaciations—Extent and Chronology*, edited by P.L. Gibbard, Elsevier, Amsterdam, 369—378.

Vieli, A., and A.J. Payne (2005), Assessing the ability of numerical ice sheet models to Simulate grounding line migration, *J. Geophys. Res.*, *110*, F01003, doi:10.1029/2004JF000202.

Walker, R.T., and D.M. Holland (2007), A two-dimensional coupled model for ice shelf-ocean interaction, *Ocean Modell.*, *17*, 123-139.

Wang, Z., and L.A. Mysak (2006), Glacial abrupt climate changes and Dansgaard-Oeschger oscillations in a coupled climate model, *Paleoceanography*, *21*, PA2001, doi:10.1029/2005PA001238.

APPENDIX A. COMPARISON OF GLACIAL AND SEA ICE CONTRIBUTION

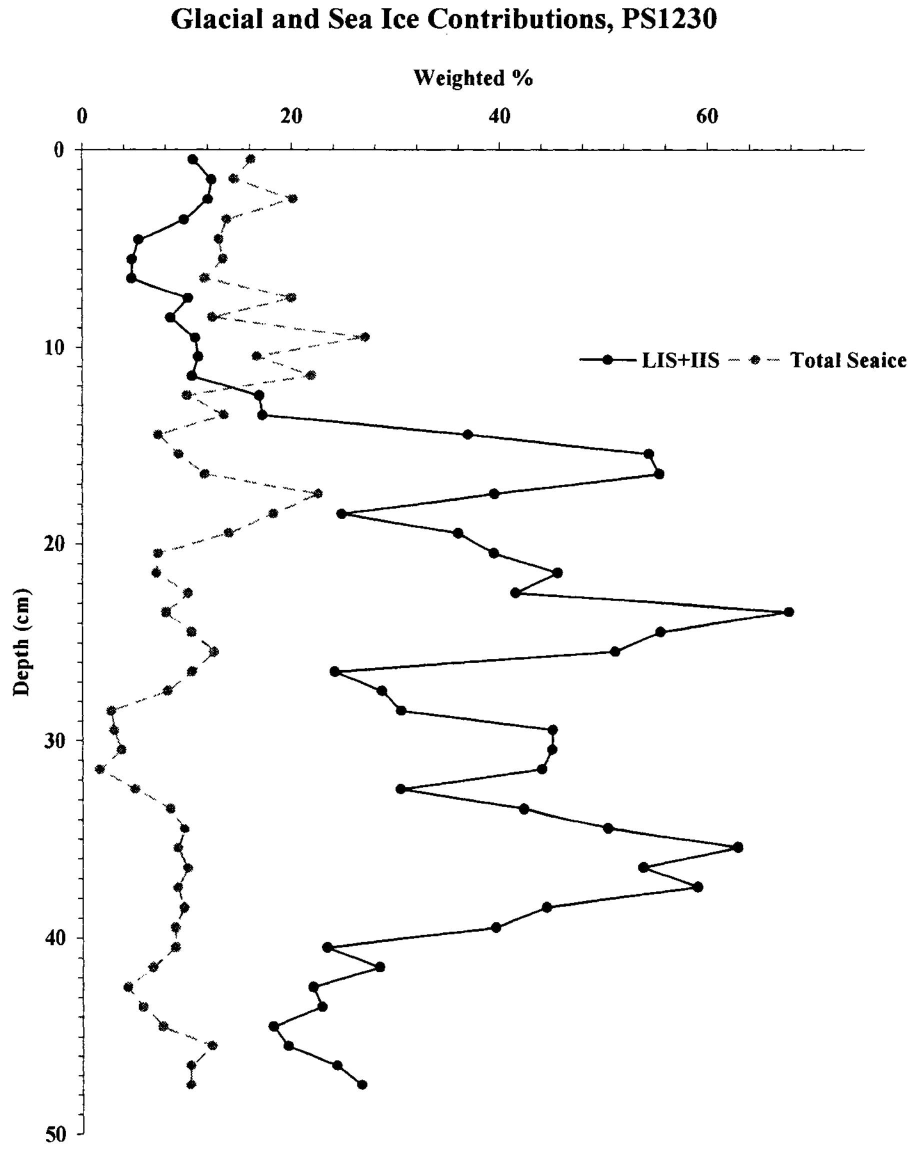

Figure 22. Contribution of glacial and sea ice to Fe grain abundances in PS1230. Note glacial and sea ice signals tend to mirror one another, suggesting a problem with closure.

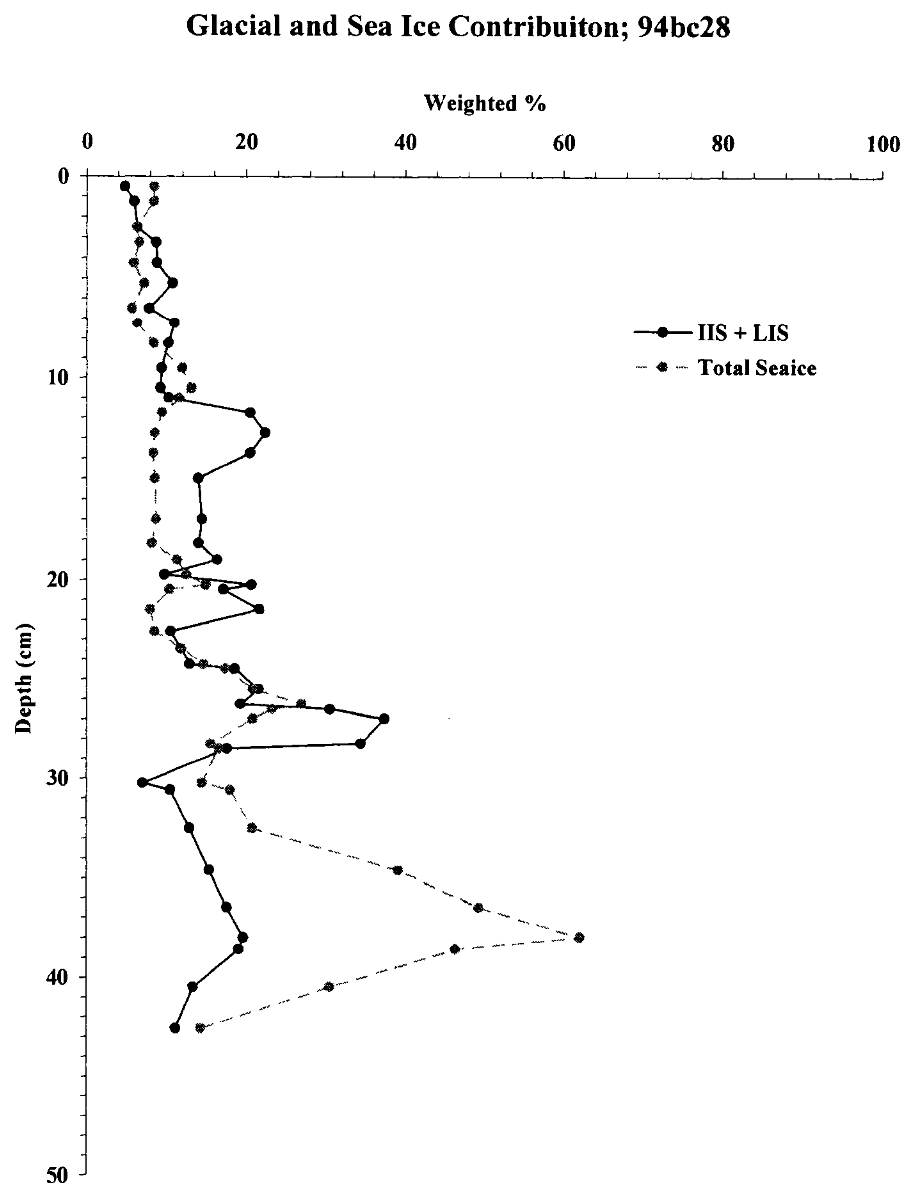

Figure 23. Contribution of glacial and sea ice to Fe grain abundances in 94BC28. Note glacial and sea ice signals tend to mirror one another, suggesting a problem with closure.

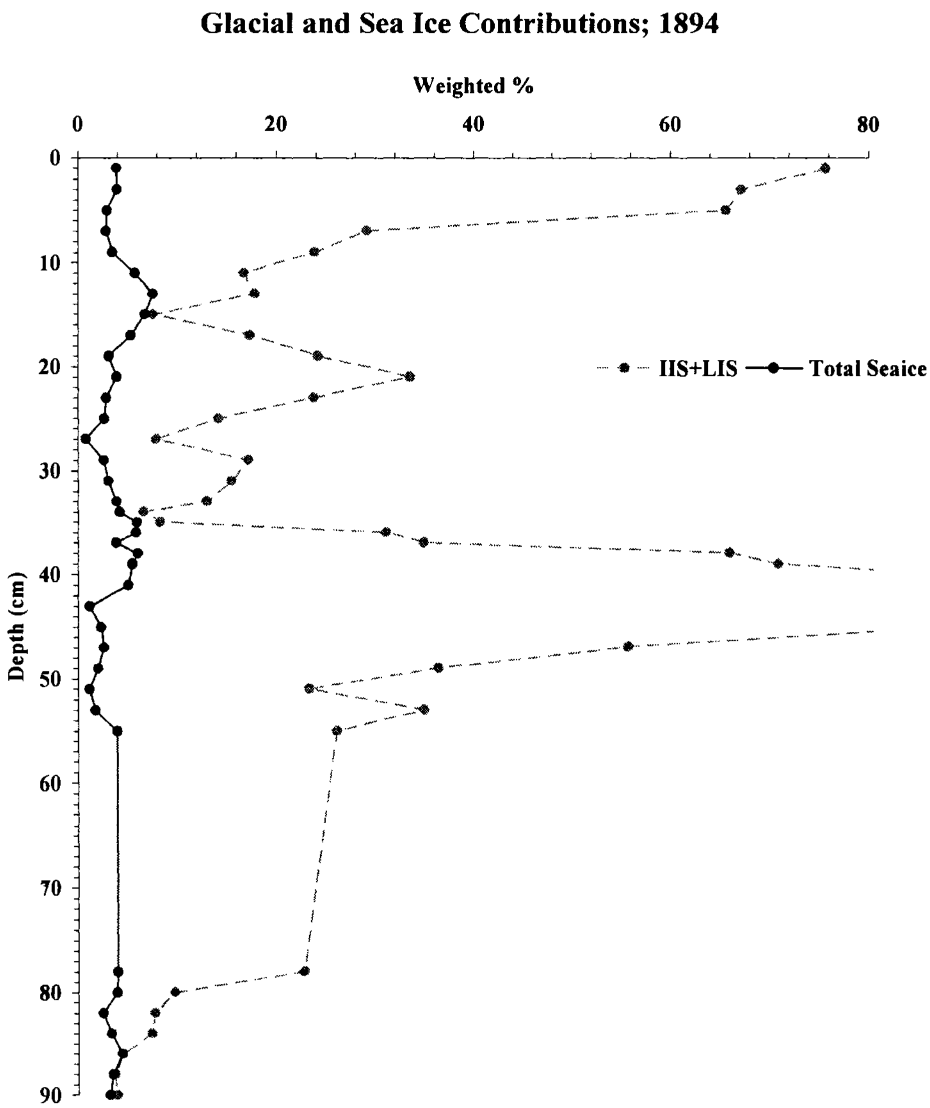

Figure 24. Contribution of glacial and sea ice to Fe grain abundances in 1894. Note glacial and sea ice signals tend to mirror one another, suggesting a problem with closure.

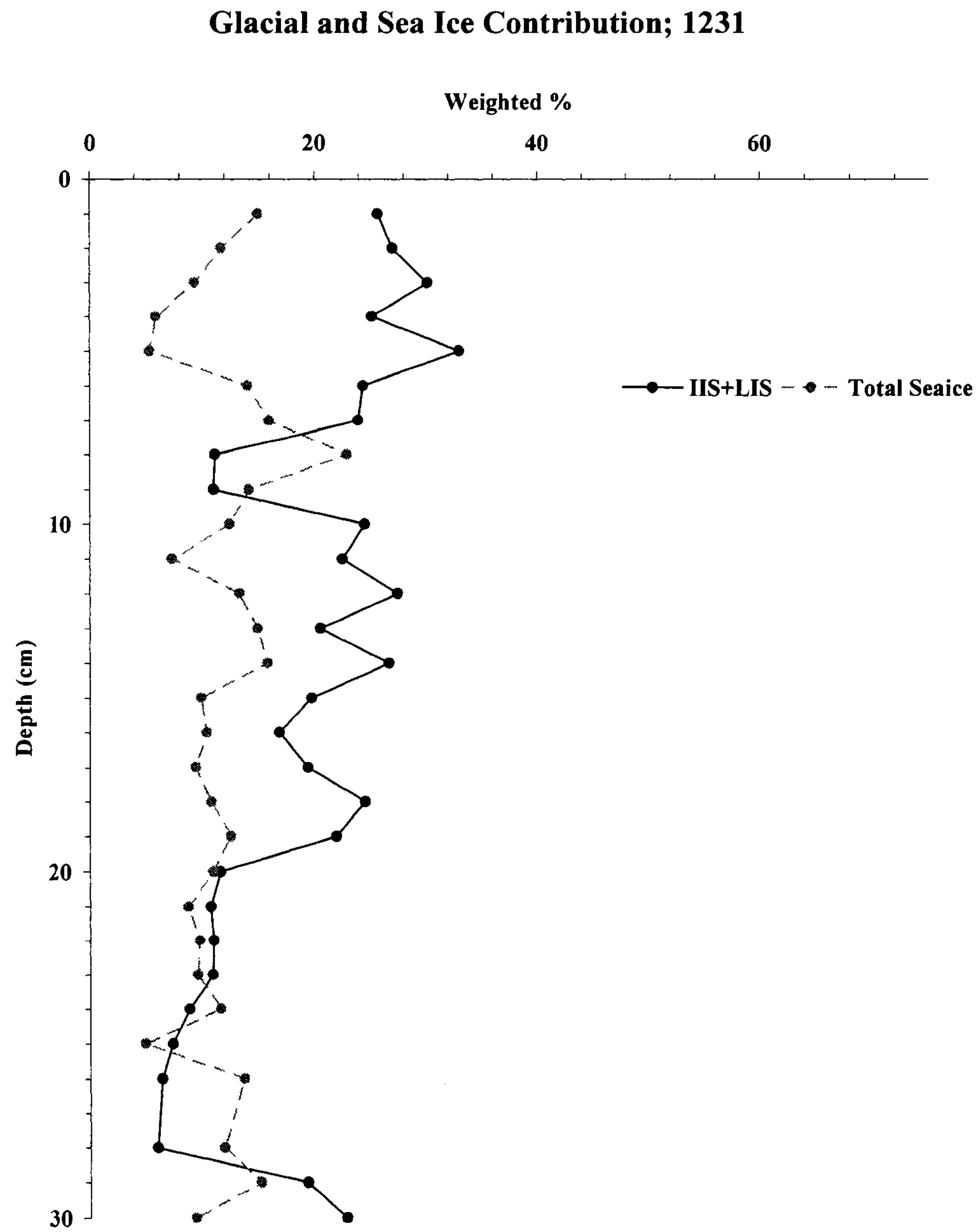

Figure 25. Contribution of glacial and sea ice to Fe grain abundances in PS1231. Note glacial and sea ice signals tend to mirror one another, suggesting a problem with closure.

APPENDIX B. SUPPLIMENTARY CORES

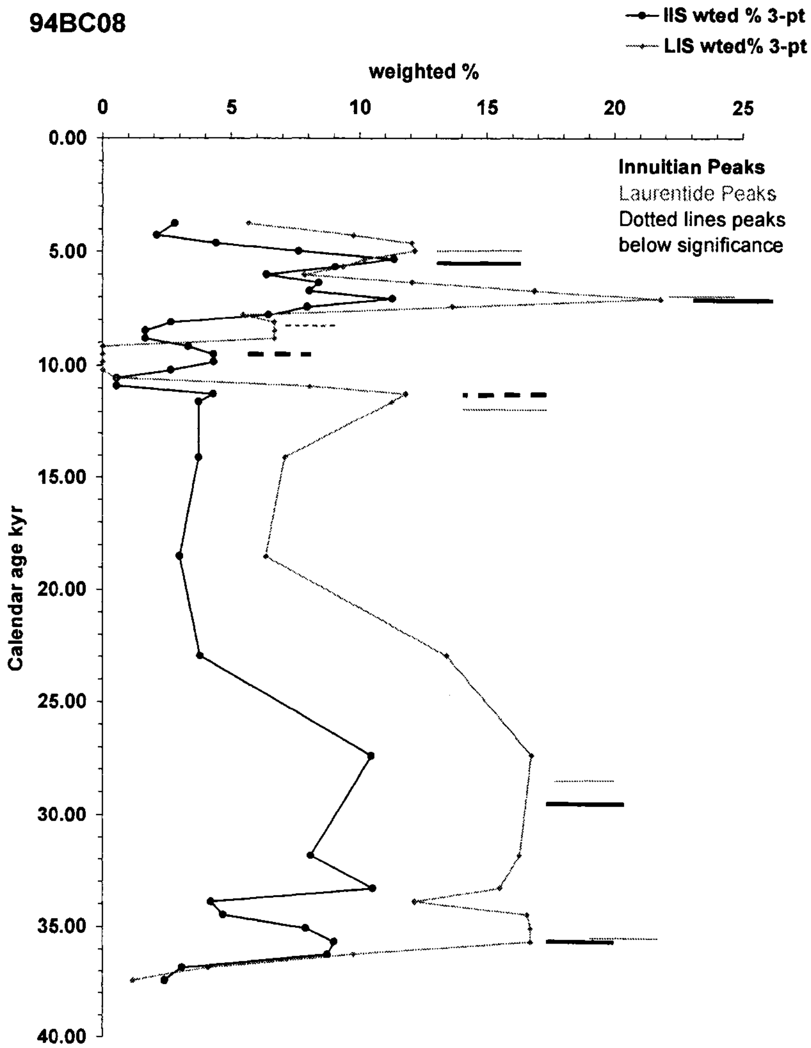

Figure 26. Fe grain weighted percents matched to the LIS and IIS in 94BC08. There is a possible IIS event around 11 ka, but this peak is below significance. The LIS event is either a lone event, or leads an insignificant IIS peak.

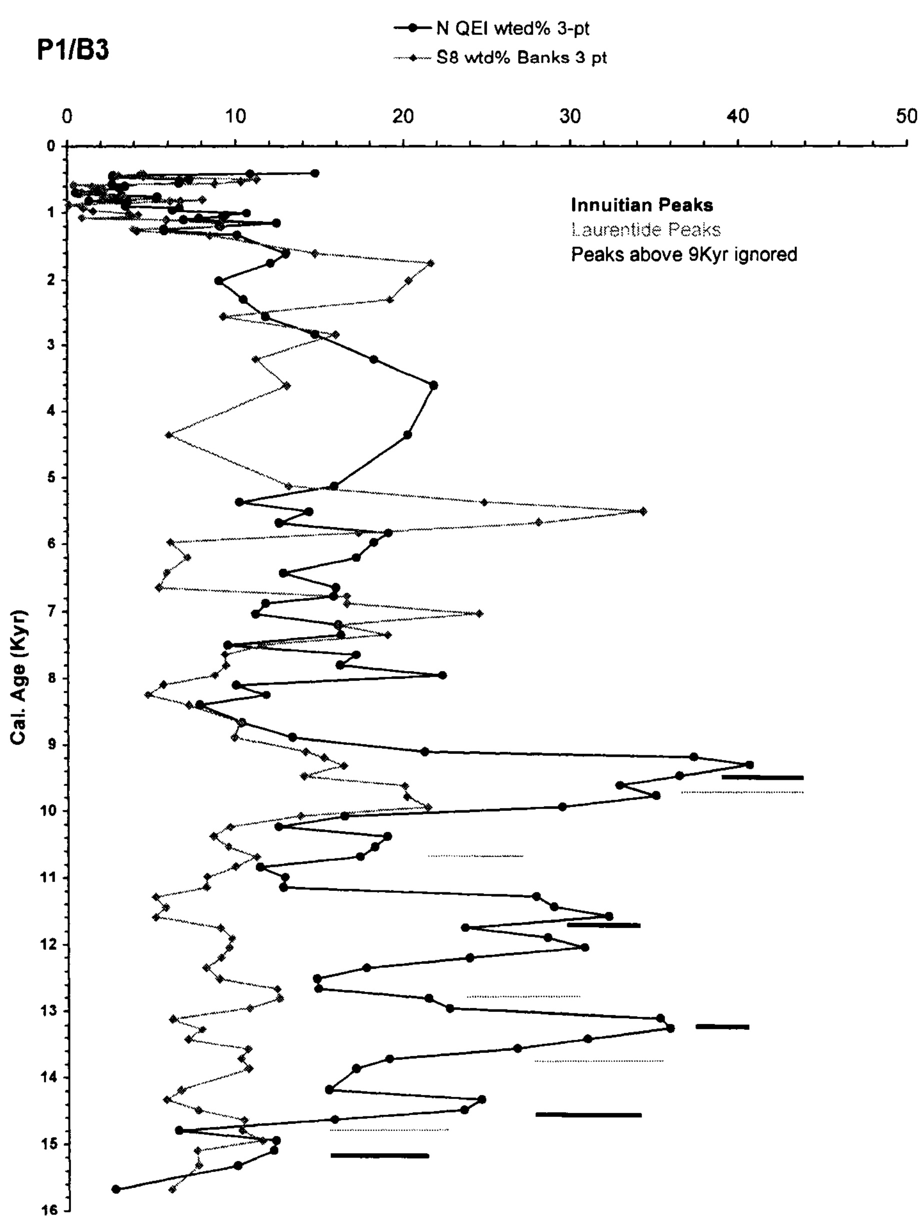

Figure 27. Fe grain weighted percents matched to the LIS and IIS in P1/B3. This core shows a mix of close and far-spaced events, making it difficult to determine if the LIS or IIS is leading.

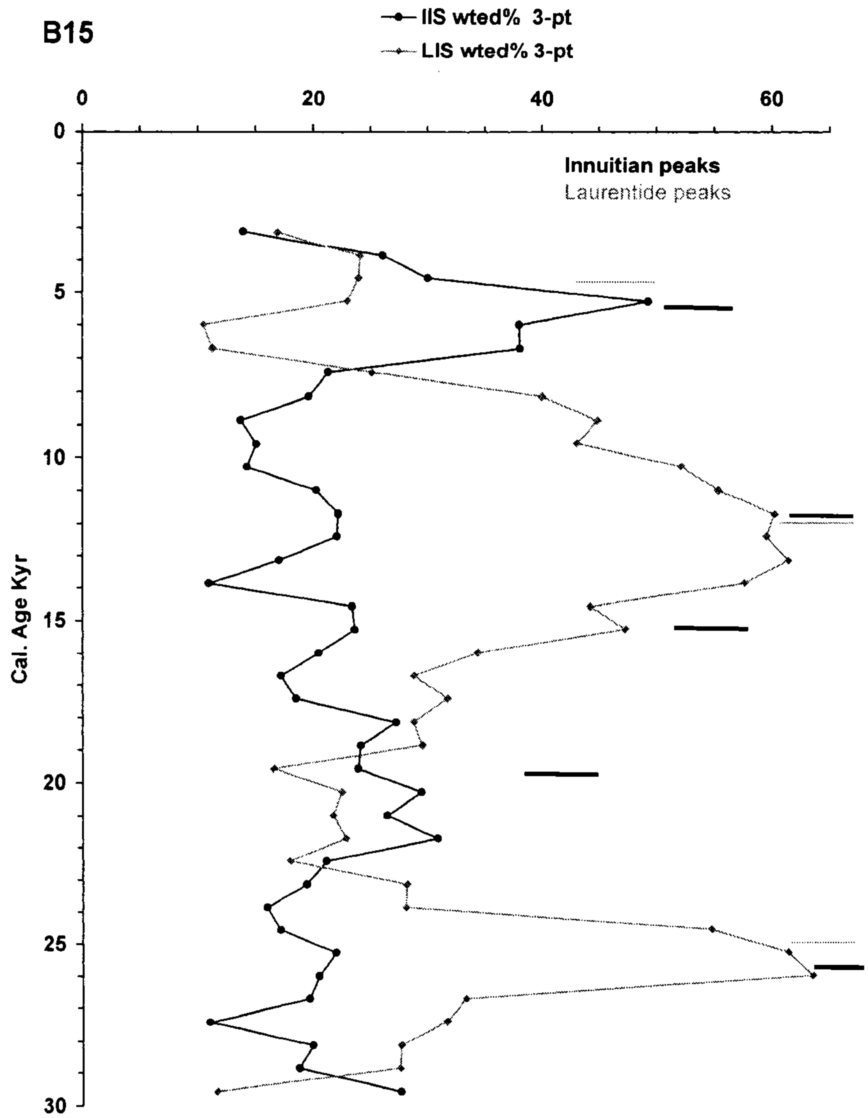

Figure 28. Fe grain weighted percents matched to the LIS and IIS in B15. Half of all events are lone IIS events.

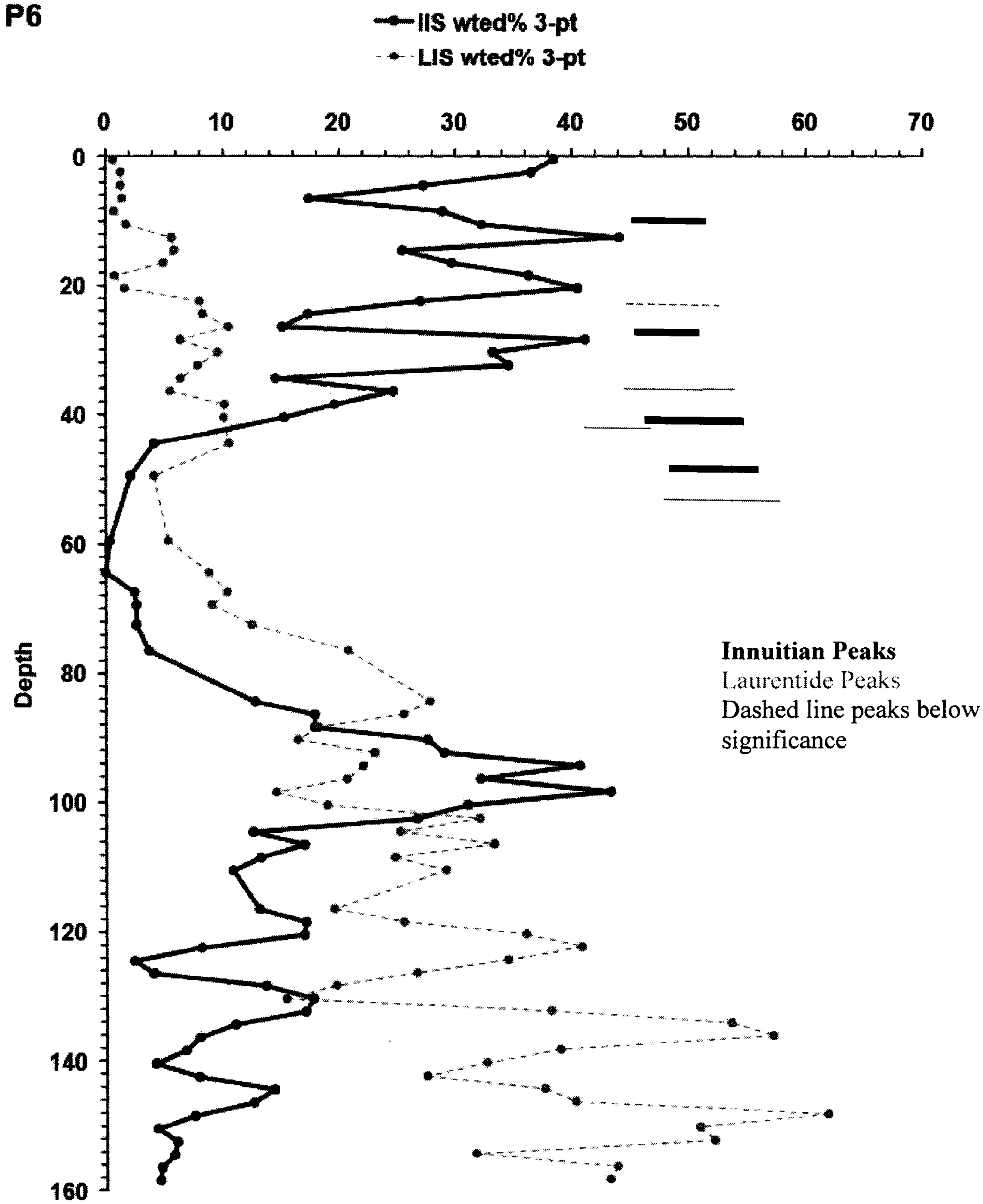

Figure 29. Fe grain weighted percents matched to the LIS and IIS in P6. During the Wisconsinan, the Laurentide weighted percents are consistently smaller than the Innuitian to a depth of 40 cm, below which point the LIS becomes dominant.

VITA

Paula Zimmerman graduated from Michigan Technological University in December 2001 with a B.S. in Geology. She is currently completing the requirements for an M.S. in Geology at Old Dominion University, in the Department of Ocean, Earth, and Atmospheric Sciences (4600 Elkhorn Ave, Norfolk VA 23529). Between graduating from MTU and applying for graduate studies at ODU, she worked as a geologist for the United States Army Corps of Engineers, Detroit District. Ms. Zimmerman is currently a staff geologist for Alkai Consultants LLC in Silverdale, Washington.